13th International "Hiroshima" Symposium on the Development and Application of Semiconductor Tracking Detectors (HSTD13)

Time resolution of single pixel irradiated 3D devices up to 10^{17} n_{eq}/cm^2 at 120 GeV SPS pion beams

Evangelos – Leonidas Gkougkousis

University of Zurich, CERN

•3D Sensors

Timing at Extreme Fluences

3D Sensors: Decoupling of charge generation and drift volume
(***Standard columns, TimeSpot, Hex geometries*** ect.)

Pros

- High radiation tolerance up to several times 10^{16} n_{eq}/cm^2
- Short drift distances with fast rise times
- Reduced Landau fluctuation, practically non-existent for perpendicular tracks

Cons

- Non-uniform field geometry
- Lower production yield
- Increased cell capacitance

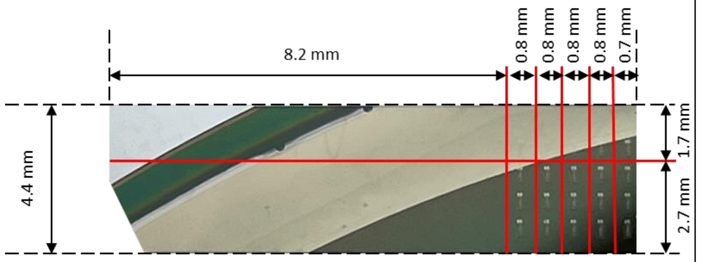

Double Sided
(thicker, more expensive)

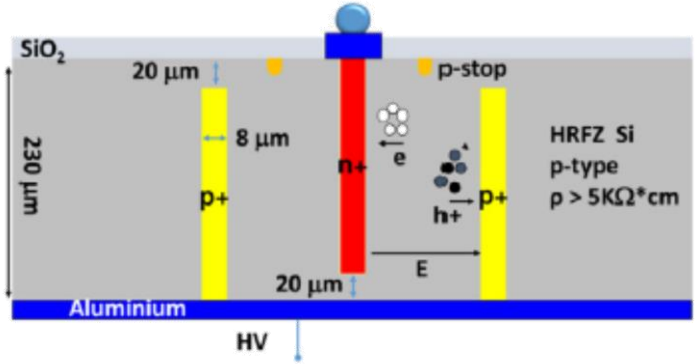

Single Sided
(thinner, simpler process)

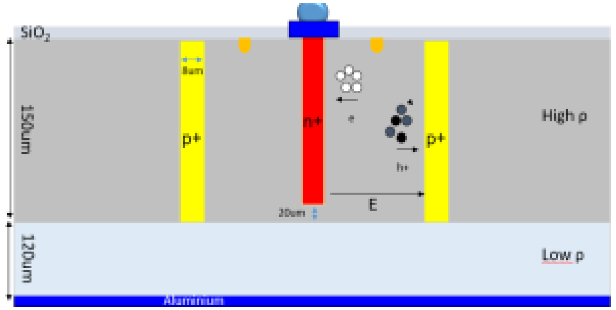

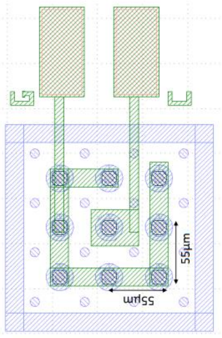

ATLAS IBL Type

Double sided n-on-p process
Active thickness 190 µm (total thickness 230 µm)
High Resistivity (> 2 kΩm × cm) Fz silicon

- ✓ Pixel Size 55 × 55 µm²
- ✓ Capacitance ~80 pF
- ✓ 10 µm column diameter
- ✓ Closest electrode distance: 19 µm

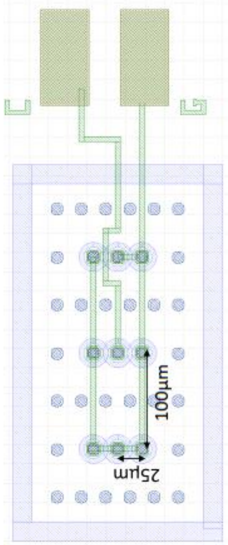

ATLeS Pre-Production type

Single sided n-on-p process
Active thickness 130 µm (total thickness 150 µm)
High Resistivity (> 2 kΩm × cm) Fz silicon

- ✓ Pixel Size 25 × 100 µm²
- ✓ Capacitance ~ 20 pF
- ✓ 8 µm column diameter
- ✓ Closest electrode distance: 35.5 µm

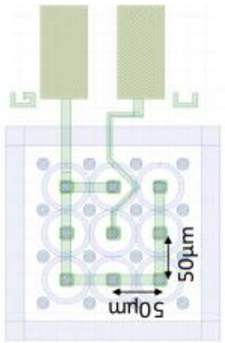

- ✓ Pixel Size 50 × 50 µm²
- ✓ Capacitance ~ 37 pF
- ✓ 8 µm column diameter
- ✓ Closest electrode distance: 19.3 µm

•3D Sensors - Timing

V. Gkougkousis, 17th Trento workshop on advanced radiation silicon detectors
"Single cell 3D timing: Time resolution assessment and Landau contribution evaluation via test-beam and laboratory measurements"

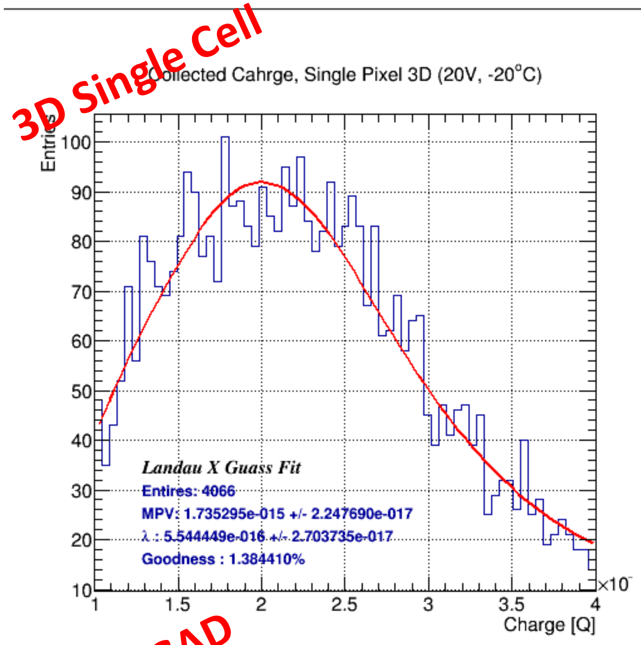

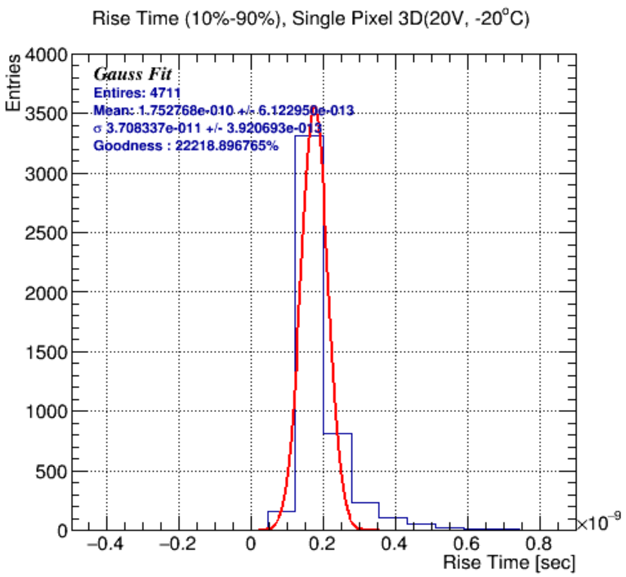

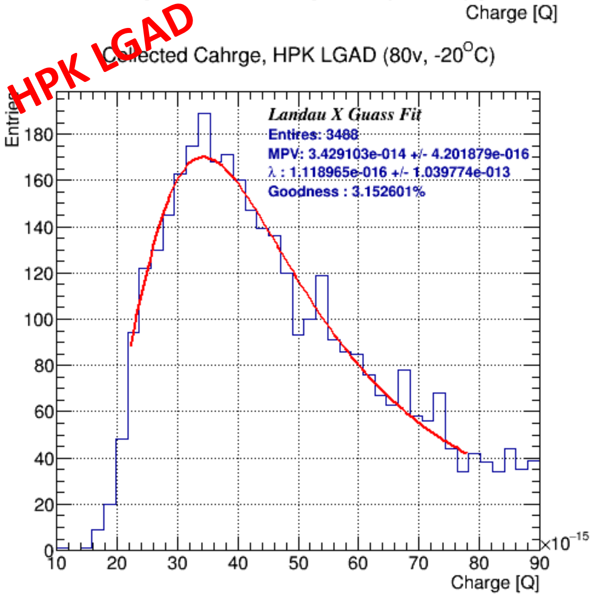

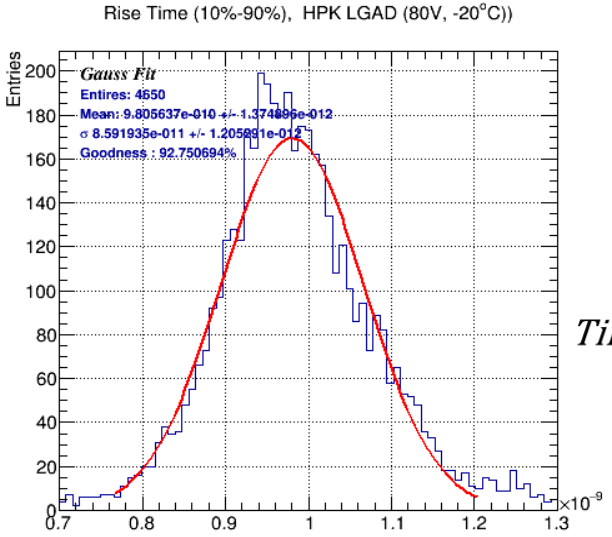

- **Extremely fast rising edge (< 180 psec)**
- **Linear stable behavior with CFD, good SNR control**

$$(\sigma_{\mathrm{Dut}})_{CFD_{ij}} = \sqrt{(\sigma^2_{\mathrm{Tot}})_{CFD_{ij}} - (\sigma^2_{\mathrm{Ref}})_{CFD_i}}$$

CFD Map, LGAD - Single Pixel 3D (-20°C, 20V)

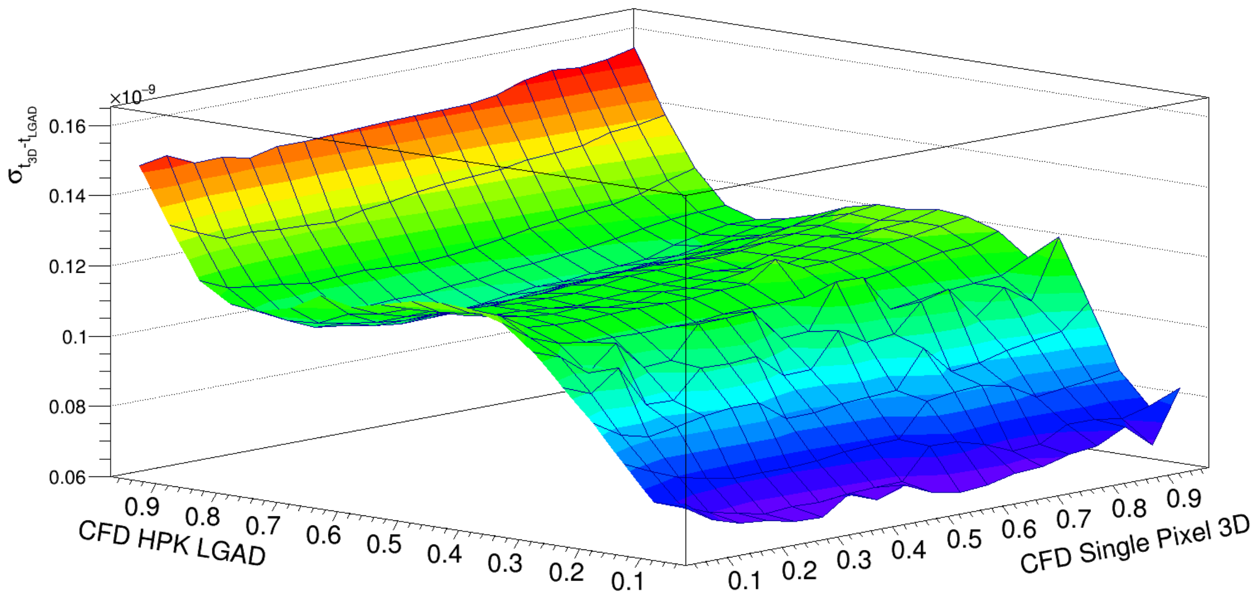

2D optimization plot – 0.5% binning

Time Resolution: $\sigma^2_{tot} = \underbrace{\sigma^2_{timewalk}}_{\sigma^2_{Dist.} + \sigma^2_{Landau}} + \underbrace{\sigma^2_{jitter}}_{\left(\frac{t_{rise}}{S/N}\right)^2} + \underbrace{\sigma^2_{conversion}}_{\left(\frac{TDC_{bin}}{\sqrt{12}}\right)^2} + \underbrace{\sigma^2_{Clock}}_{\text{Fixed Term} \sim 5\text{-}7\ psec}$

•3D Sensors – Signal Integrity

- Frequency of radioactive decay events follows Poisson law
- Record trigger time and convert to event frequency

Poisson Distribution: $f(n) = \mu^{n} * \frac{e^{-\mu}}{n!}$

Where: ***n*** number of events in interval
μ *mean*
f(n) *frequency*

$n' = n * C$

Variable change

$\mu = B/C$

$f(n') = A * \left(\frac{n'}{C}\right)^{B/C} * \frac{e^{-B/C}}{\Gamma\left(\frac{n'}{C} + 1\right)}$

Where: ***A*** Normalization parameter
B/C *mean*
f(n') *Scaled frequency*

- Efficiency dependent on bandwidth
- Signal distribution in the Fourier domain highly depends on bias
- Minimum time over threshold effect for trigger latching of instrument affect efficiency

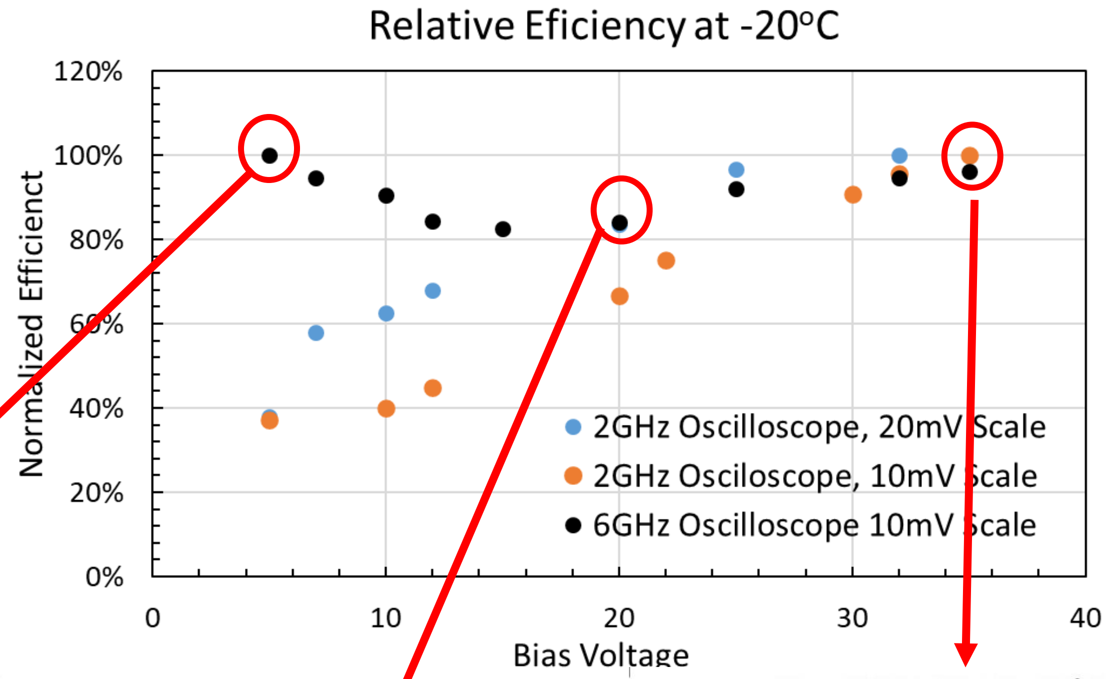

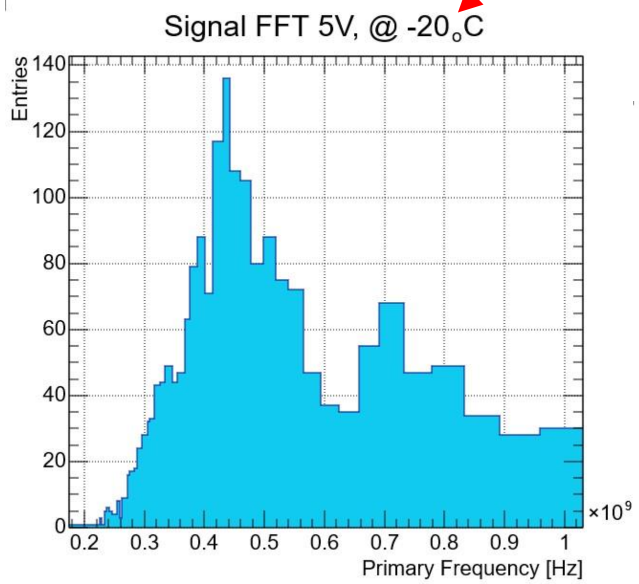

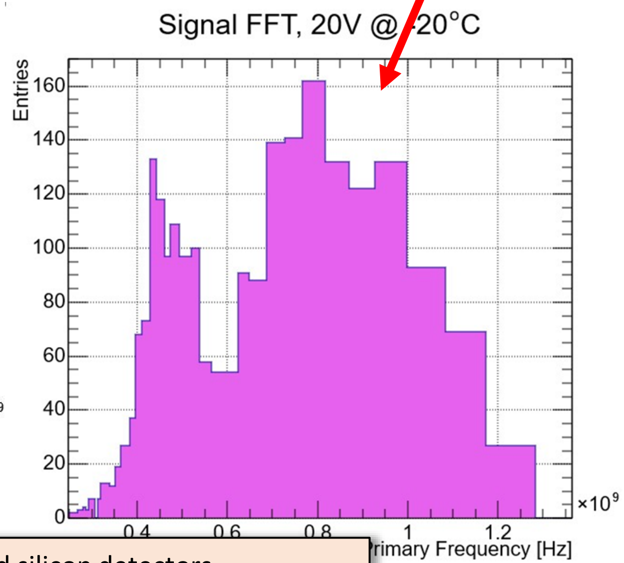

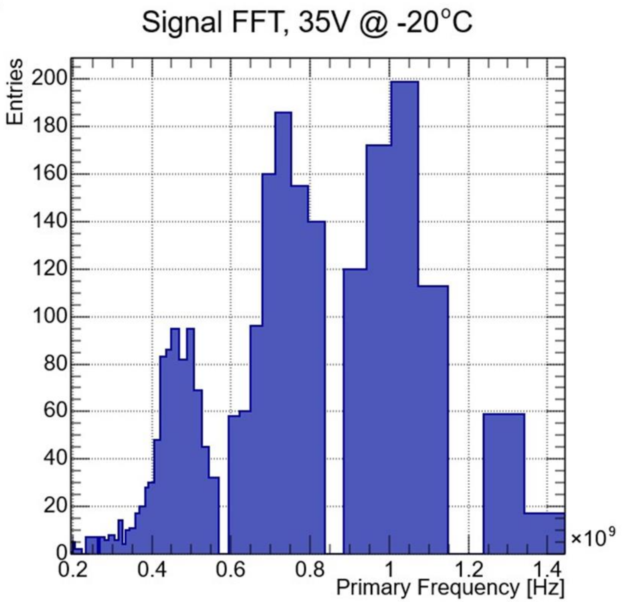

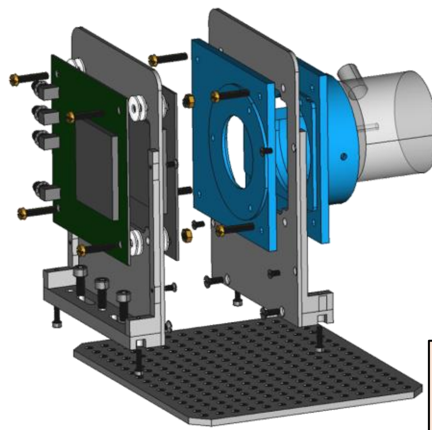

V. Gkougkousis, 35th RD50 workshop on radiation hard silicon detectors
"Efficiency estimation on irradiated LGAD with respect to sensor stability"

•Planar Sensors

Sensors: CERN EP-R&D n-on-p planar sensor run with ADVACAM at 50, 100, 200 and 300 μm active thickness

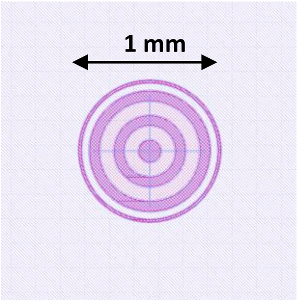

Small Diode

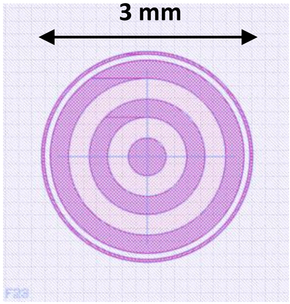

Big Diode

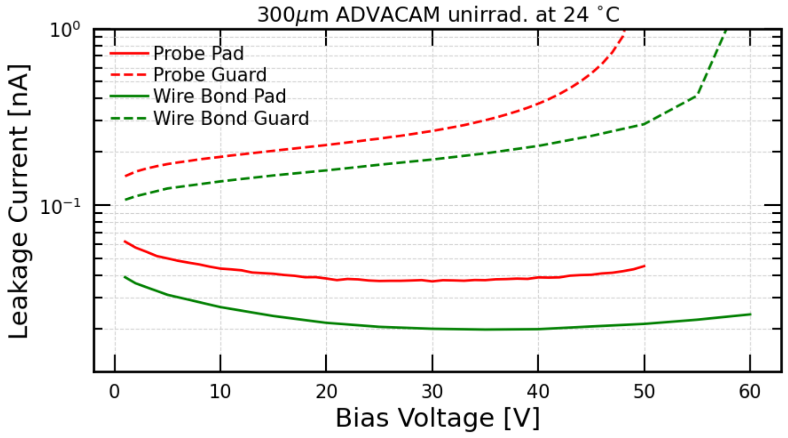

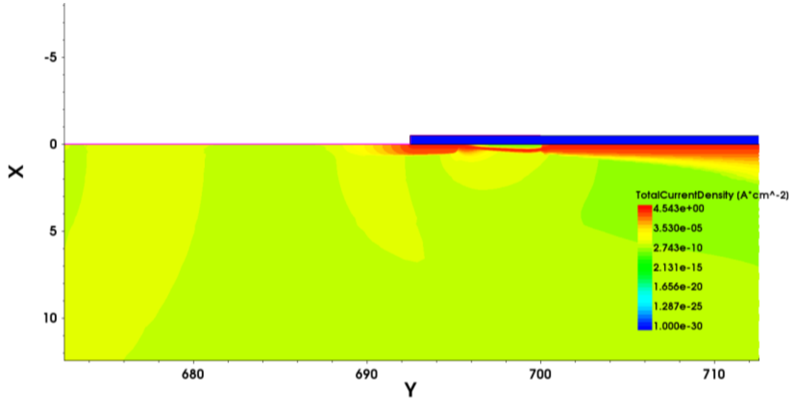

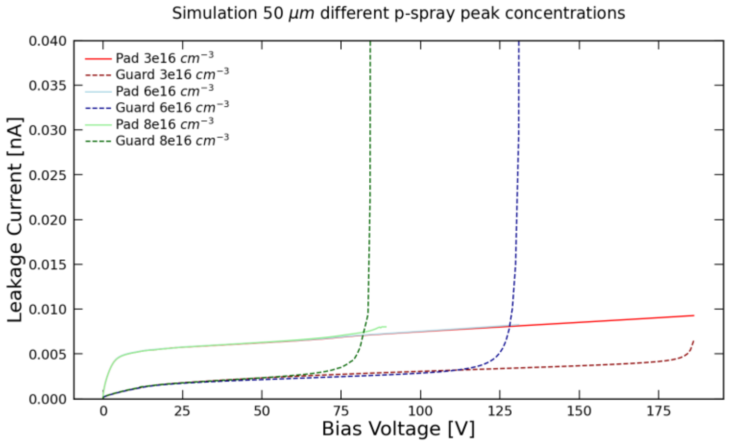

Test Structures

- Small diodes (3.14 mm2 active area) Circular diodes for timing studies due to lower capacitance
- Big diodes (28.27 mm2 active area) Circular diodes for radiation damage studies
- 5x5 Pixel matrix (0.003 mm2 active area) for charge sharing and interpixel efficiency – timing studies

Issues

- Early breakdown due to high p-spray concentration leading to impact ionisation at the interface between p-spray and electrode implant
- Breakdown first visible in guard ring due to bigger interface region compared to pad

Irradiations

(both 3D and planar)

Neutron @ JSI (Ljubljana)

- ✓ 1×10^{15} n_{eq}/cm^2
- ✓ 8×10^{15} n_{eq}/cm^2
- ✓ 6×10^{16} n_{eq}/cm^2
- ✓ 1×10^{17} n_{eq}/cm^2

Proton @ PS

- ✓ 1×10^{15} n_{eq}/cm^2
- ✓ 8×10^{15} n_{eq}/cm^2
- ✓ 6×10^{16} n_{eq}/cm^2
- ✓ 1×10^{17} n_{eq}/cm^2

•Part I - Test Beams

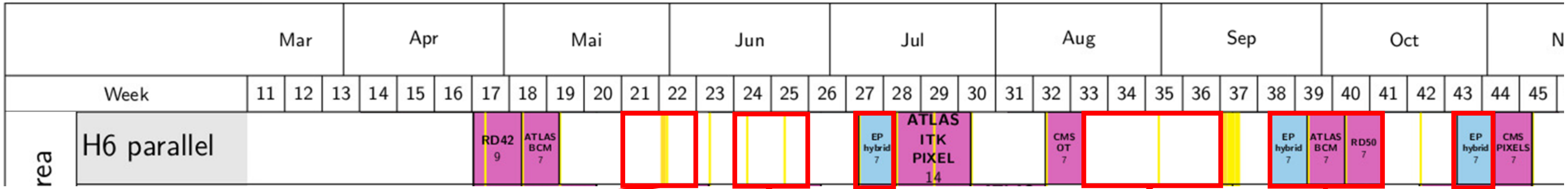

Primary user
Parallel user
Parasitic user

25 May – 8 June
15 – 29 June
6 July – 13 July
17 August - 14 September
21 September - 12 October
26 October – 2 November

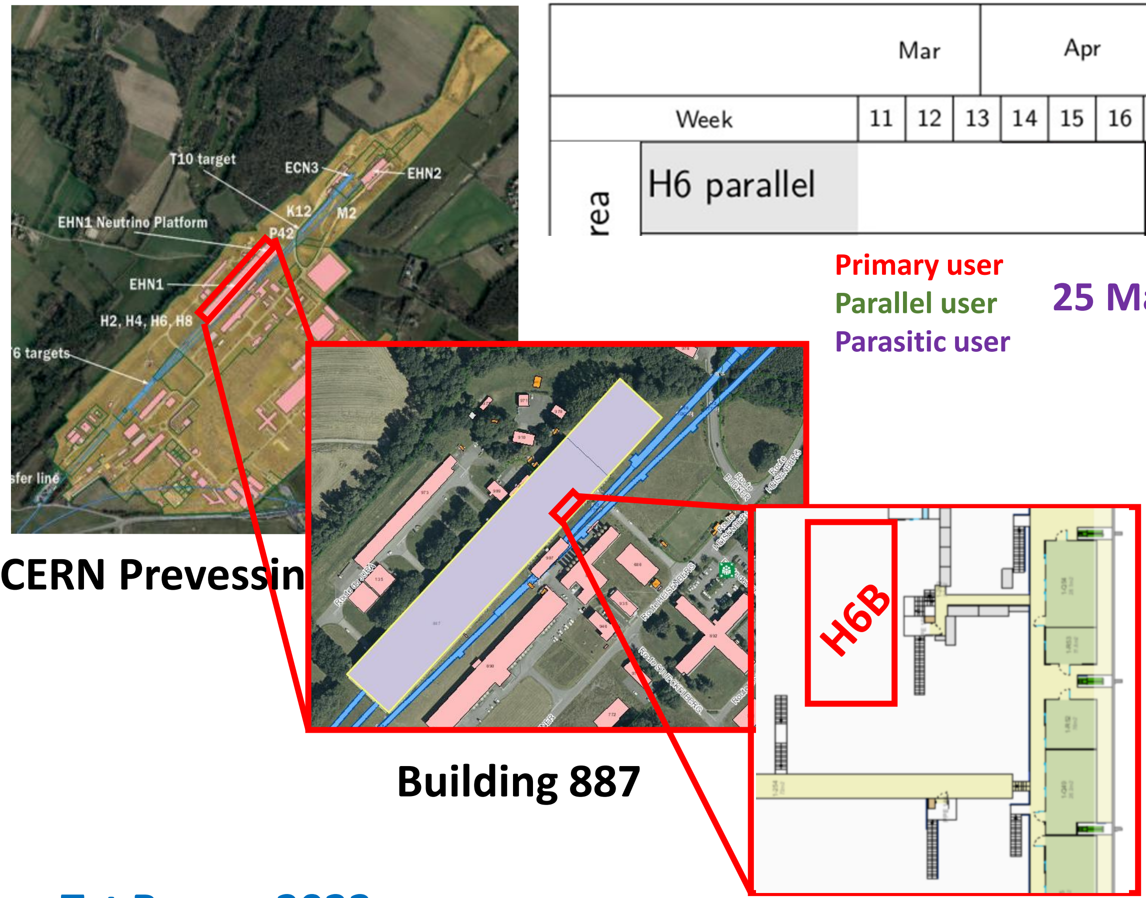

CERN Prevessin

Building 887

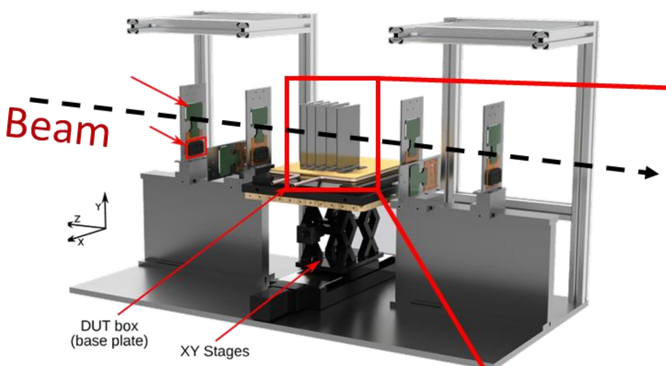

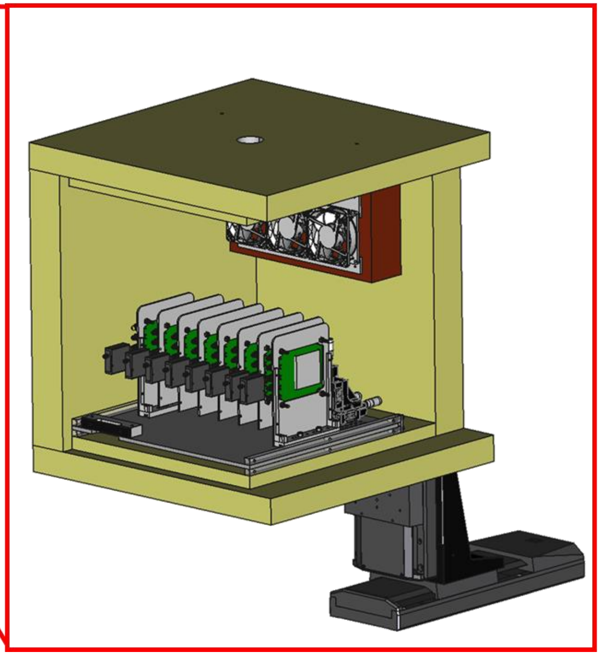

Tet Beams 2022

- Several periods but only two as primary user
- Main target irradiated Planar / 3D sensors
- No / Limited possibility of extension
- Extensive infrastructure developments

The Setup

- AIDA Telescope
- Custom Cold Box
- DUTs on individual motorized individual stages
- Pixelated alignment & ROI plane

•Test Beam Configuration

V. Gkougkousis, 40th RD50 Workshop on Radiation hard semiconductor devices for very high luminosity colliders
"Time resolution of single cell 3D devices on SPS pion beams"

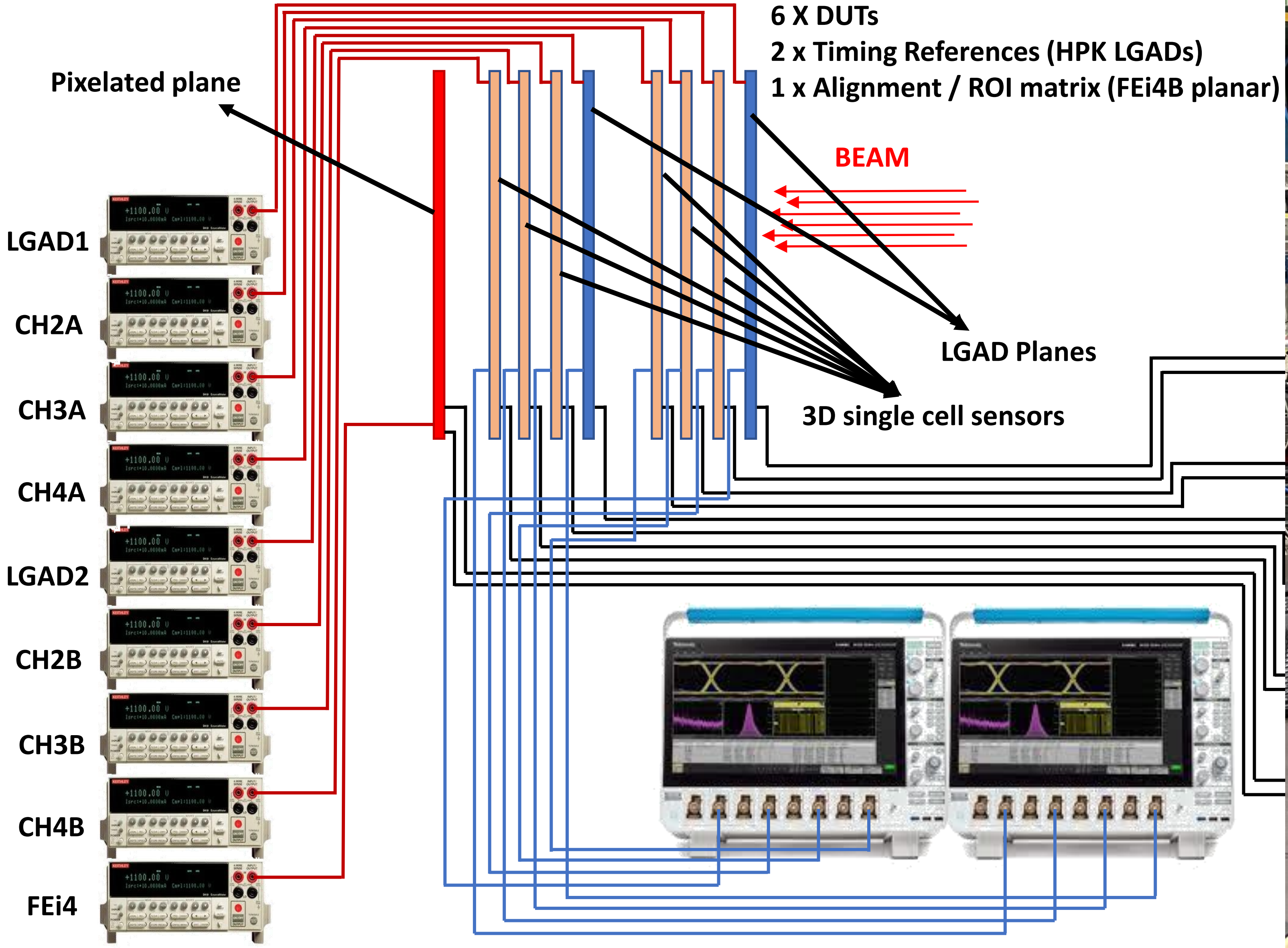

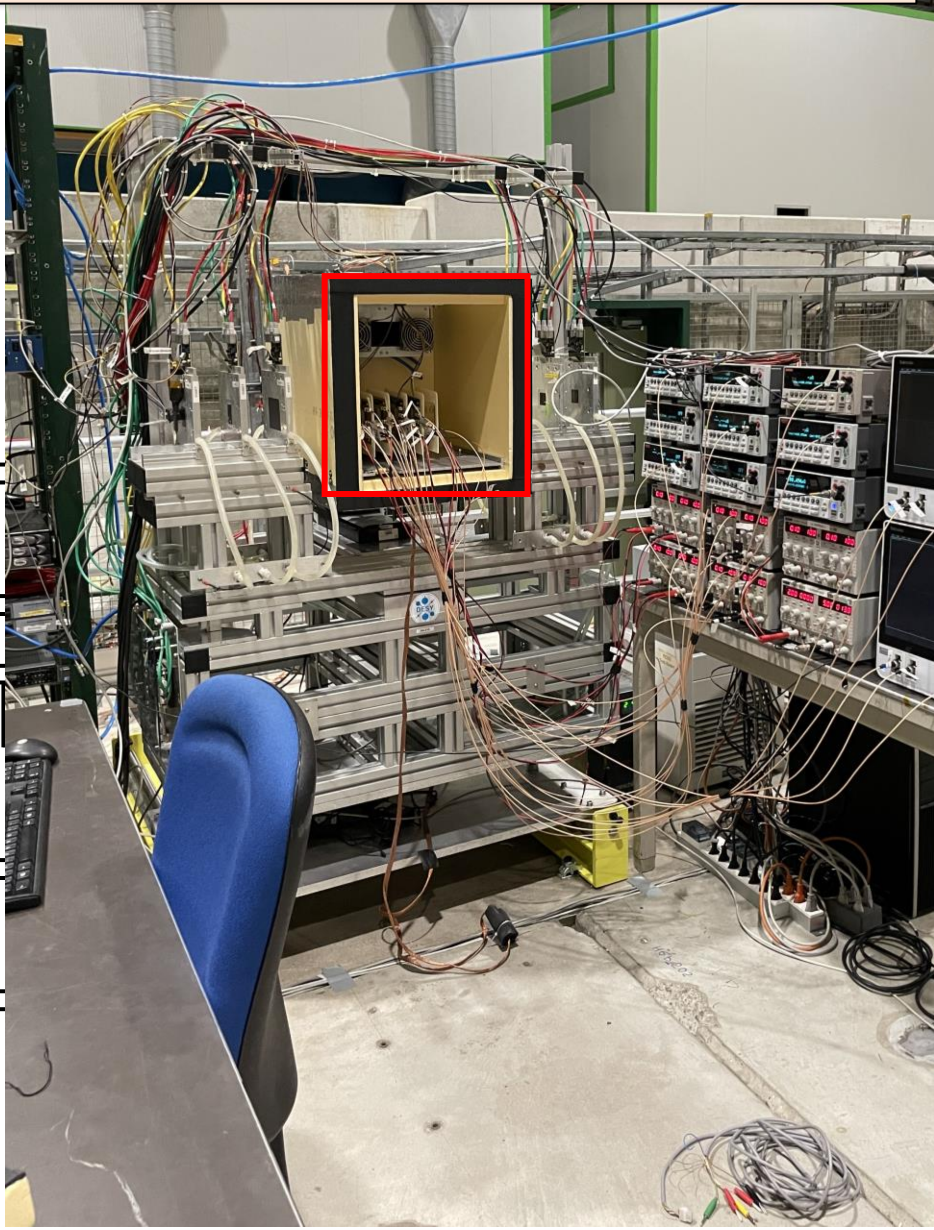

•Alignment & Mechanics

HPK LGAD Timing references

- Coincidences between DUTs and LGADs required for timing
- Alignment crucial to increase data efficiency
- Efficiency defined by largest overlapping region
- Micrometric on-line alignment using projections on FEi4 matrix
- ROI defined in addition to other trigger conditions

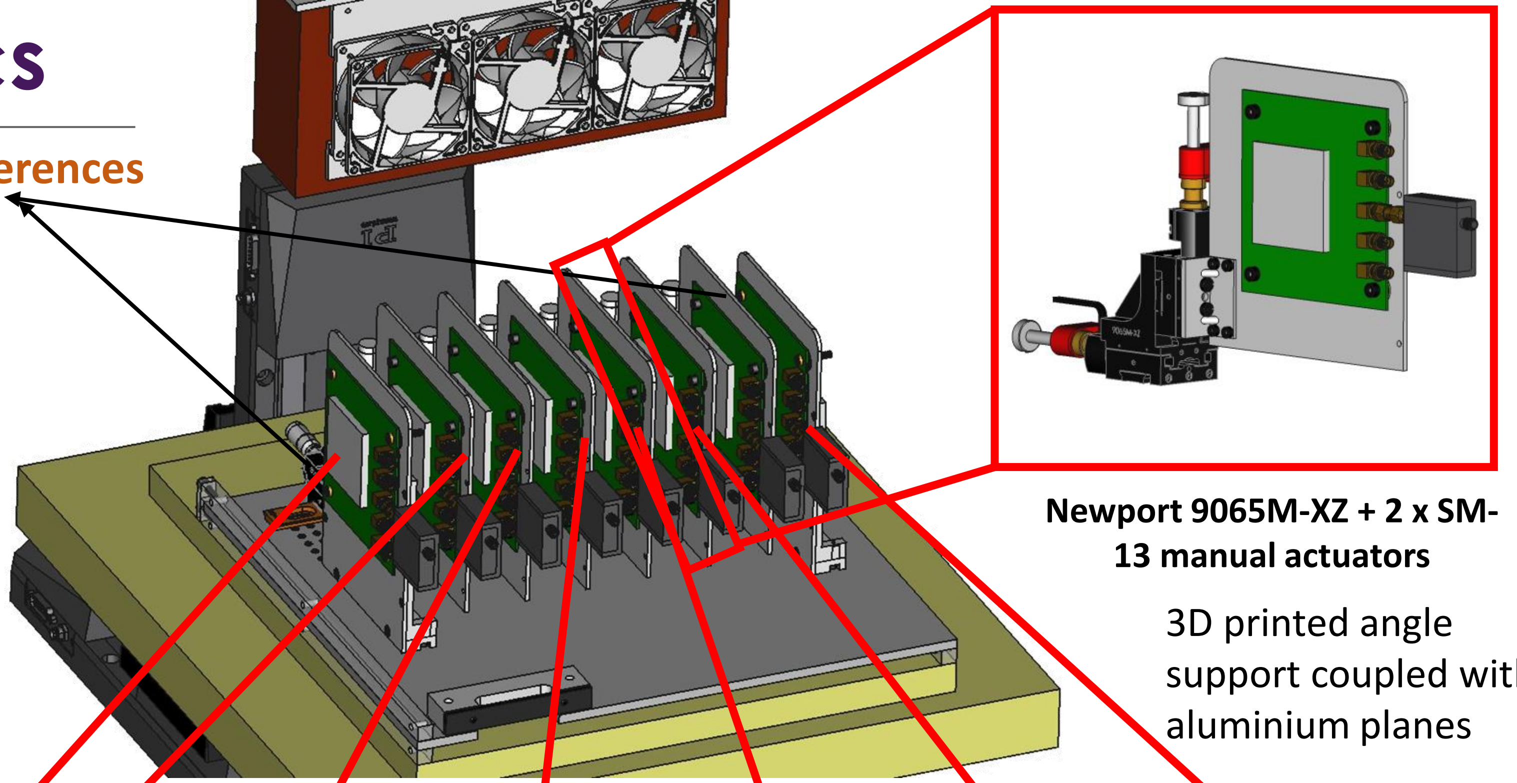

Newport 9065M-XZ + 2 x SM-13 manual actuators

3D printed angle support coupled with aluminium planes

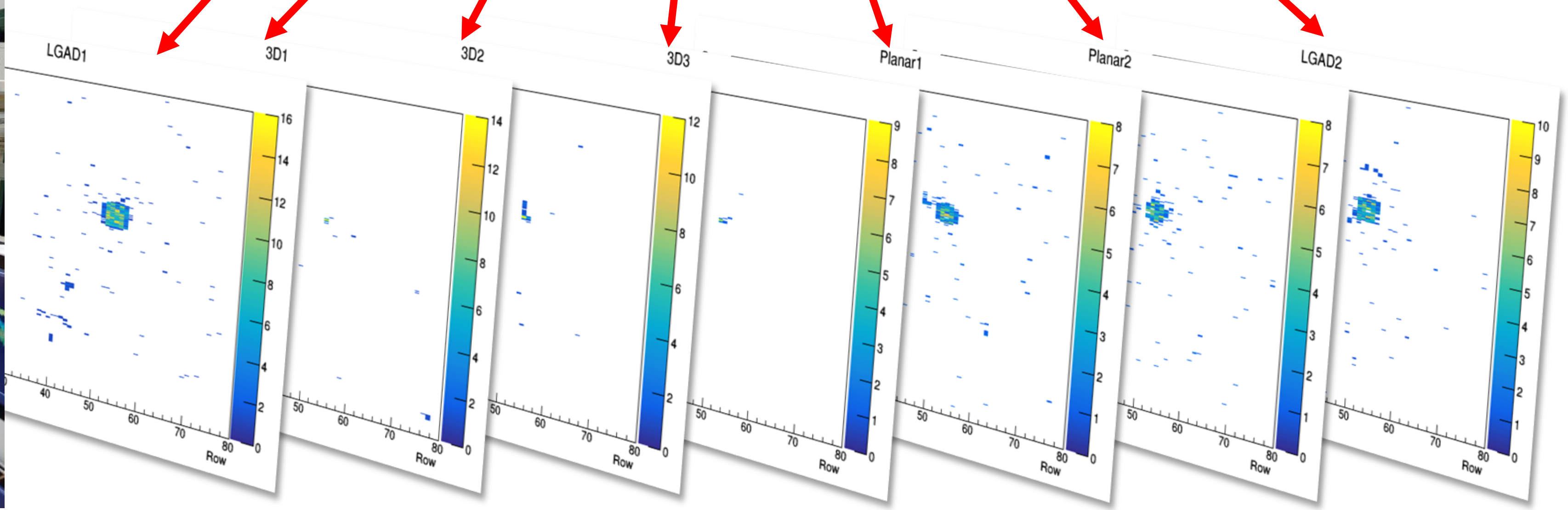

•Trigger Interface Board (TiB)

- Oscilloscope in fast readout mode with binary format
- Event readout only between SPS-spills or when event buffer full ti increase efficiency
- TLU Synchronization by vetoing data taking during read-out
- RJ-45 or HDMI for EUDET TLU communication (EUDET 2 compatible)
- **Versatile design**, I/Os **Reconfigurable** and microcontroller **Reprogrammable** via USB

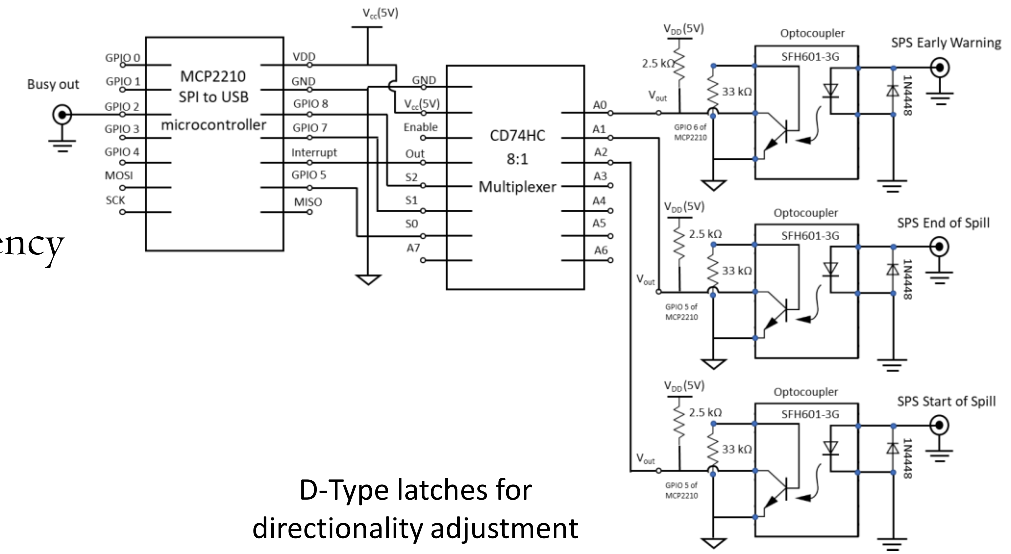

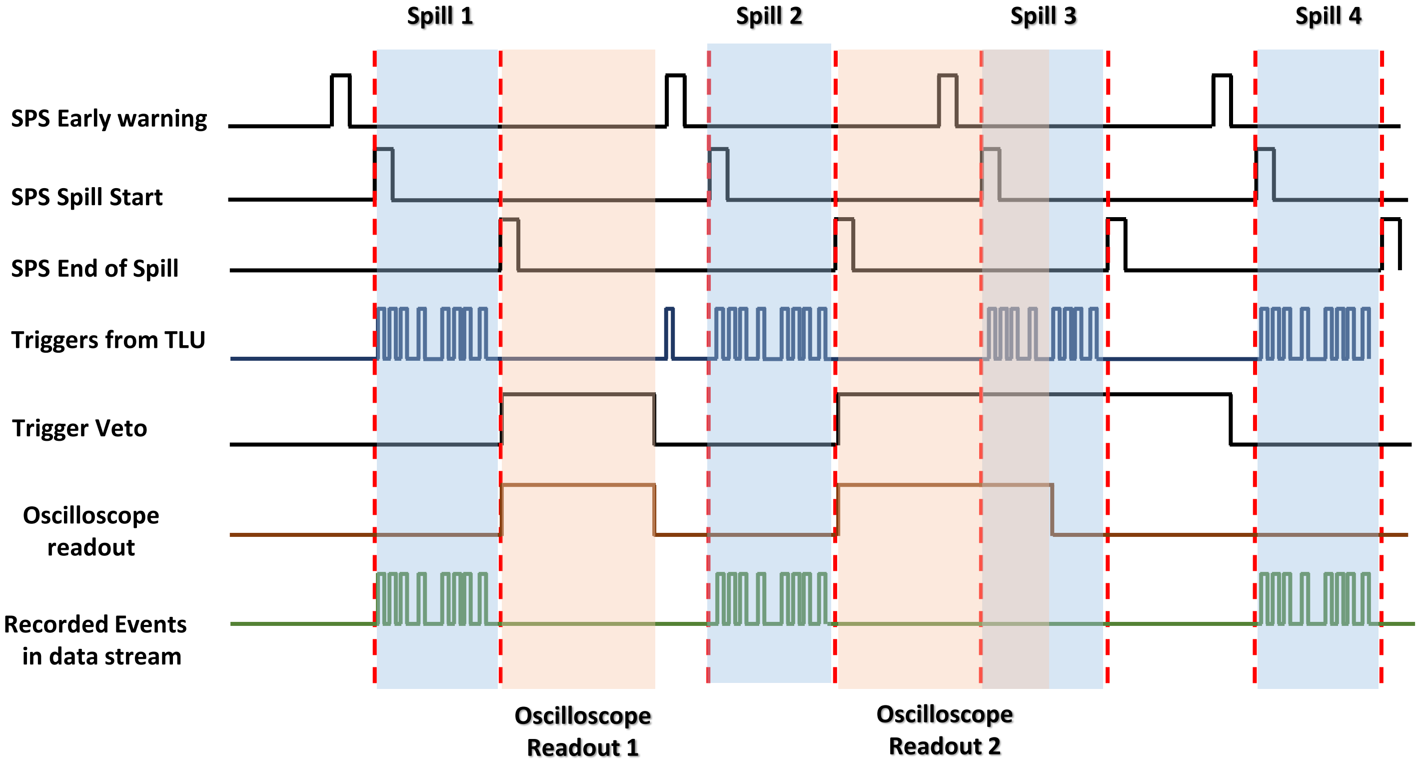

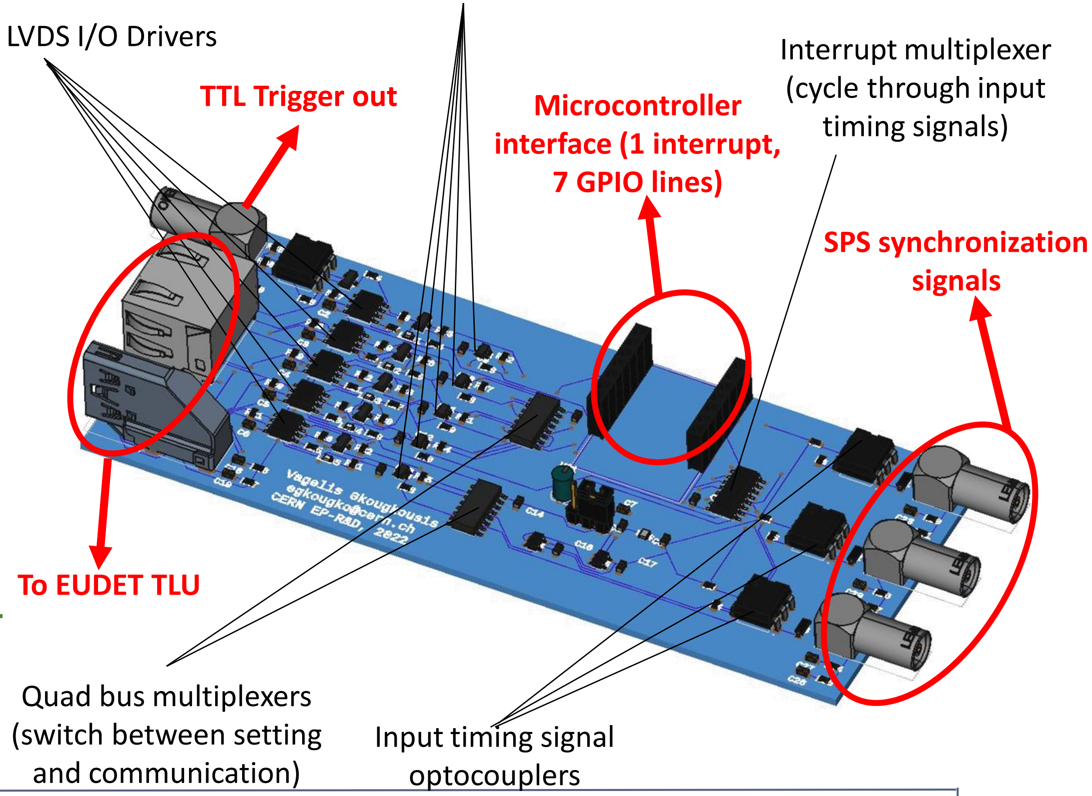

•Tracking and ROI

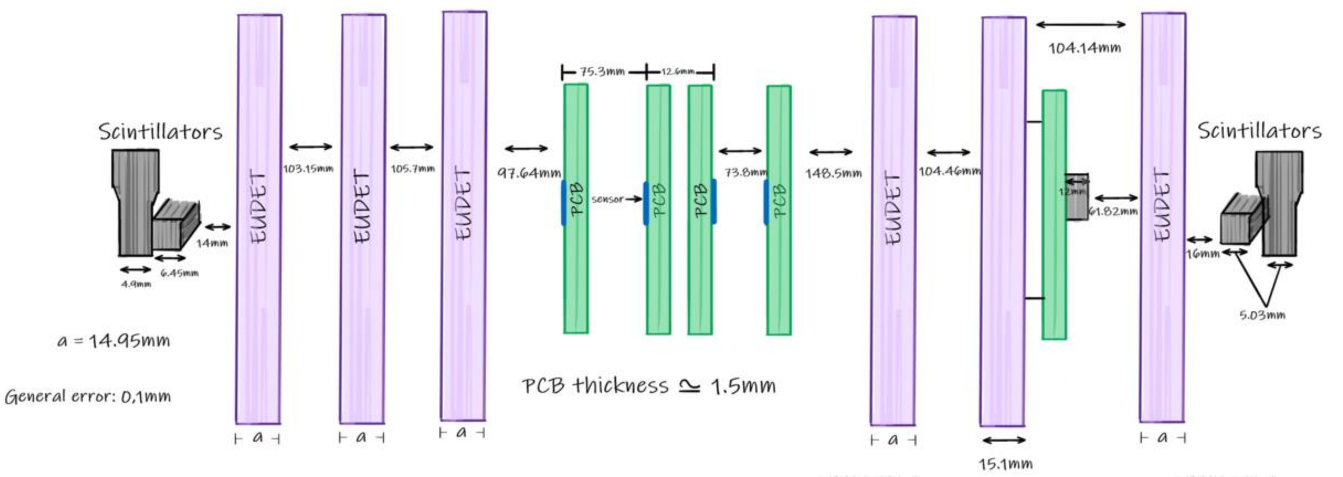

Telescope Planes

- **6 MIMOSA planes for tracking**
- **Plane no. 5 known to be bad**
- **5 μm – 7 μm tracking resolution**
- **Estimated acquired number of events ~1M**

- Limited beam control as parasitic user
- Suffer from low intensity and low data rates of EUDAQ

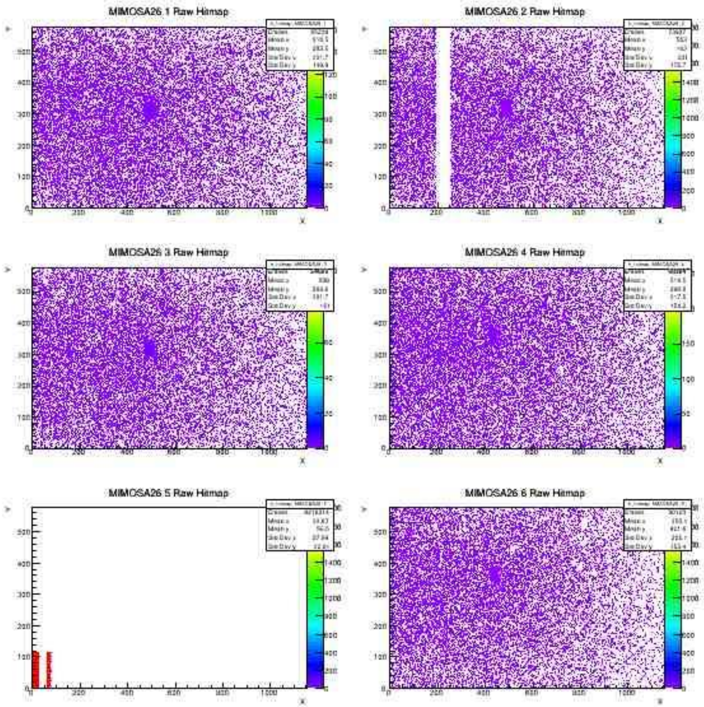

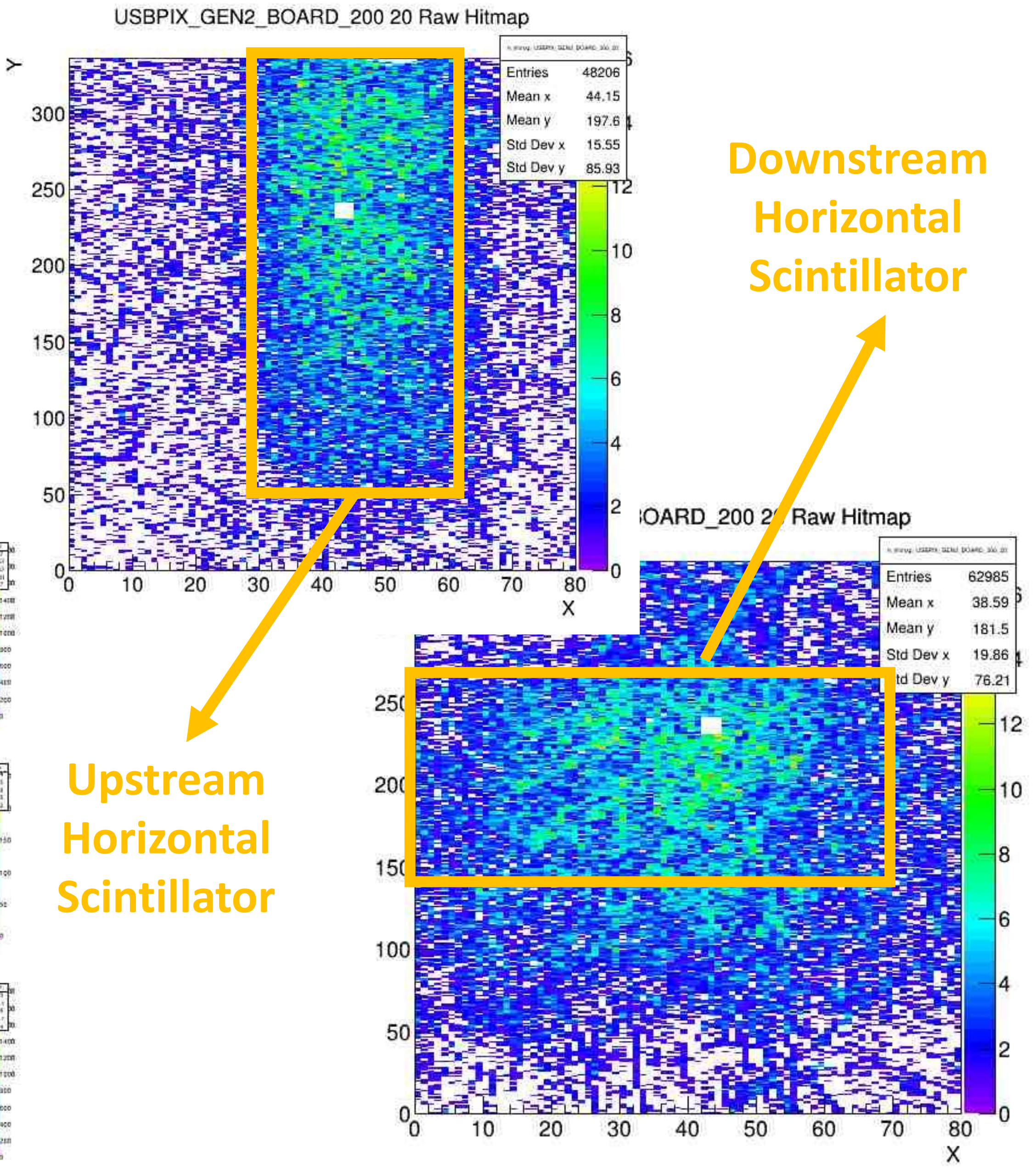

•The importance of bandwidth

V. Gkougkousis, Ultrafast imaging and tracking Instrumentation, Methods and Applications Conference - ULITIMA 2023
"[Radiation damage effects overview on Low Gain Avalanche Diodes]"

LGADs

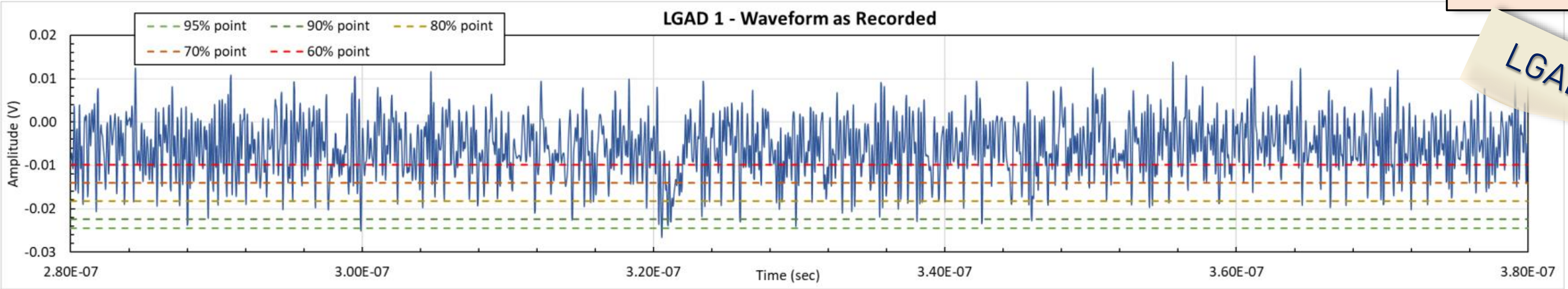

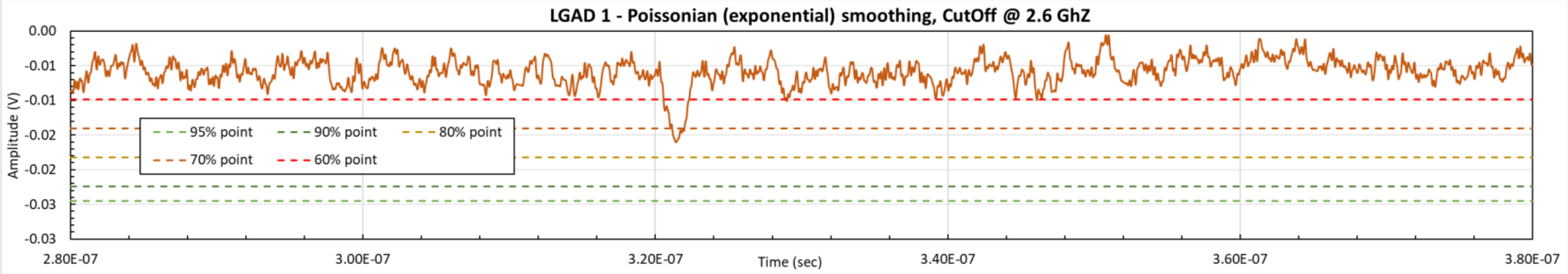

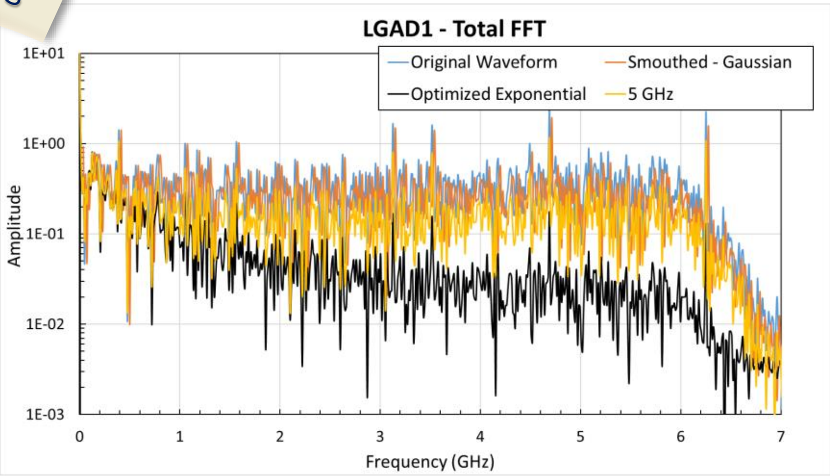

3Ds

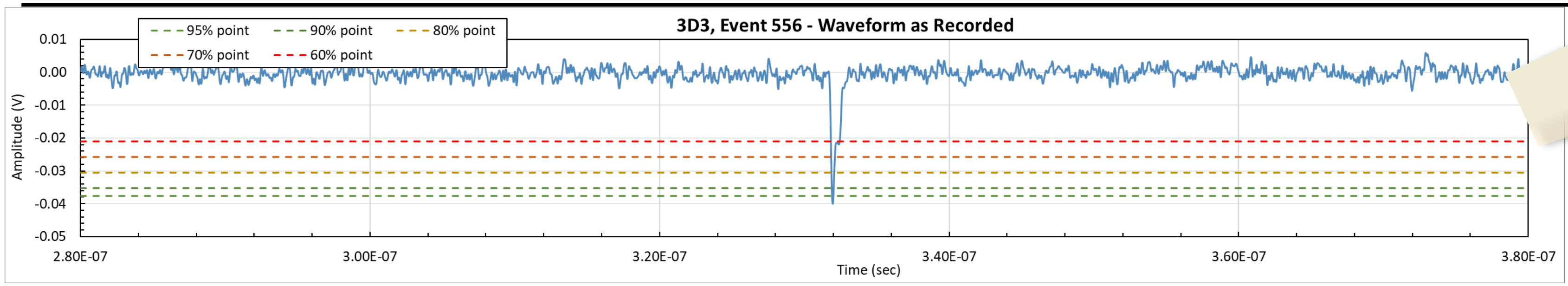

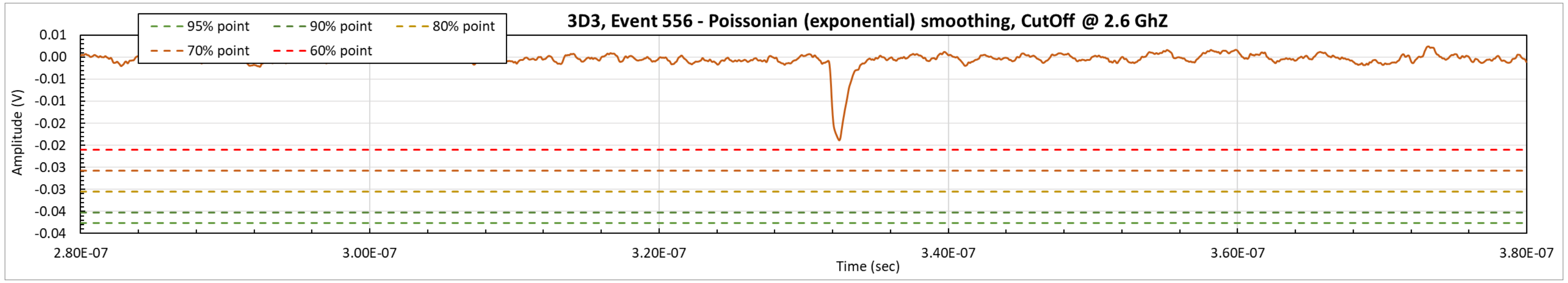

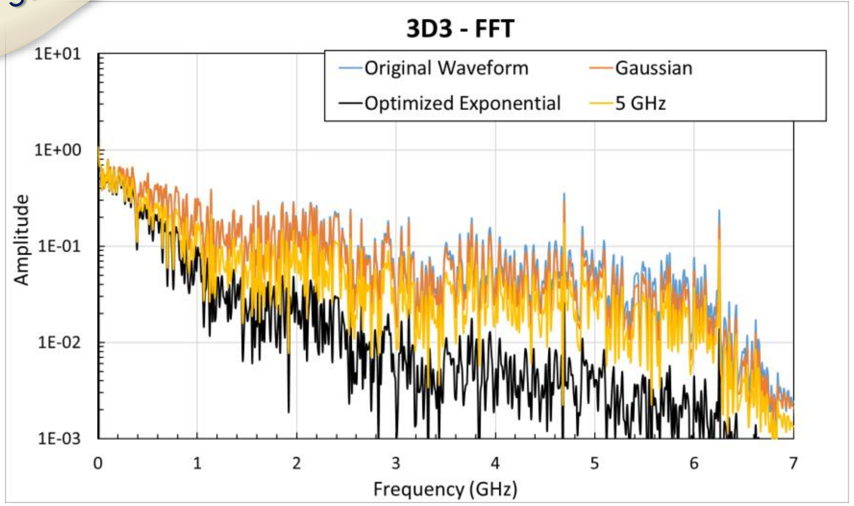

•The importance of bandwidth

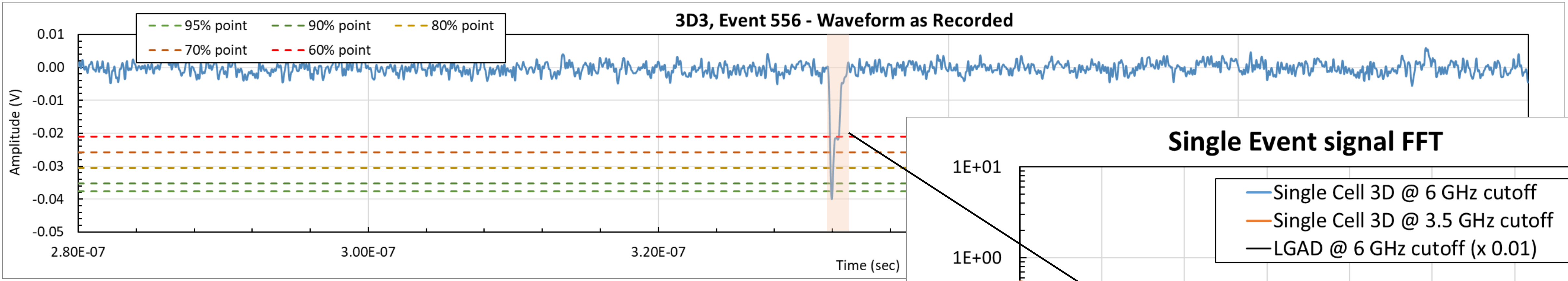

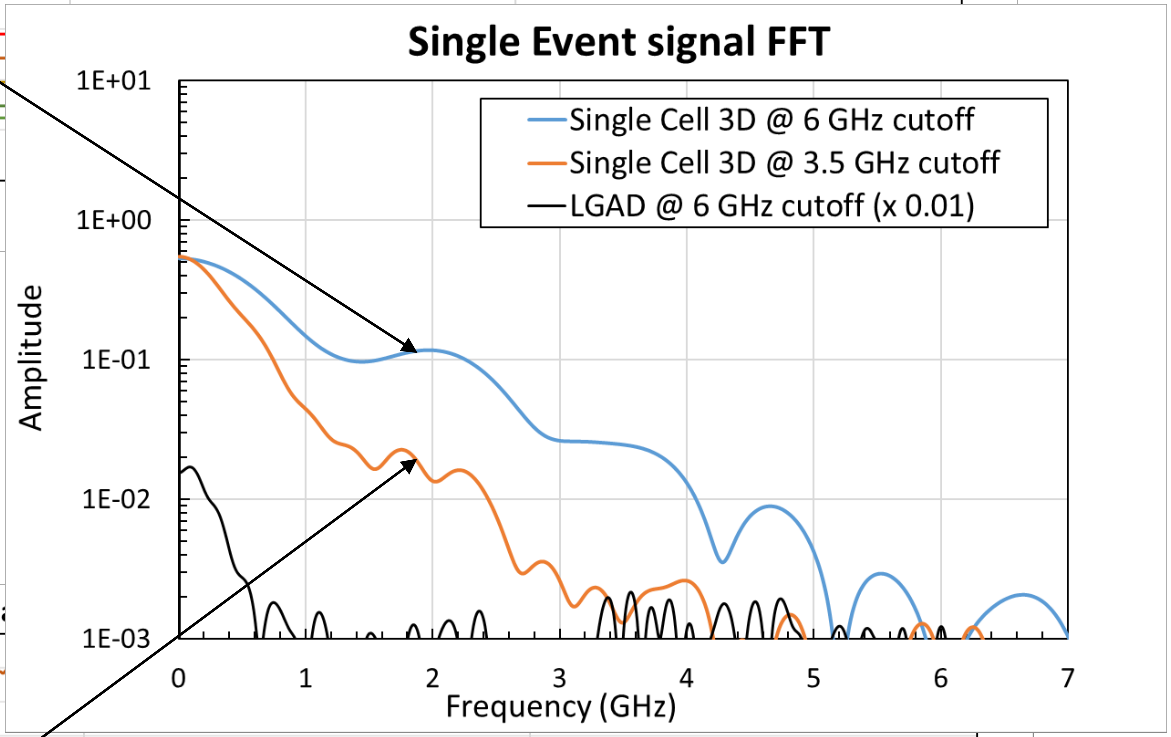

- **60 % less amplitude**
- **20 % more charge**
- **If bandwidth not correct, we are probing electronics transfer function**

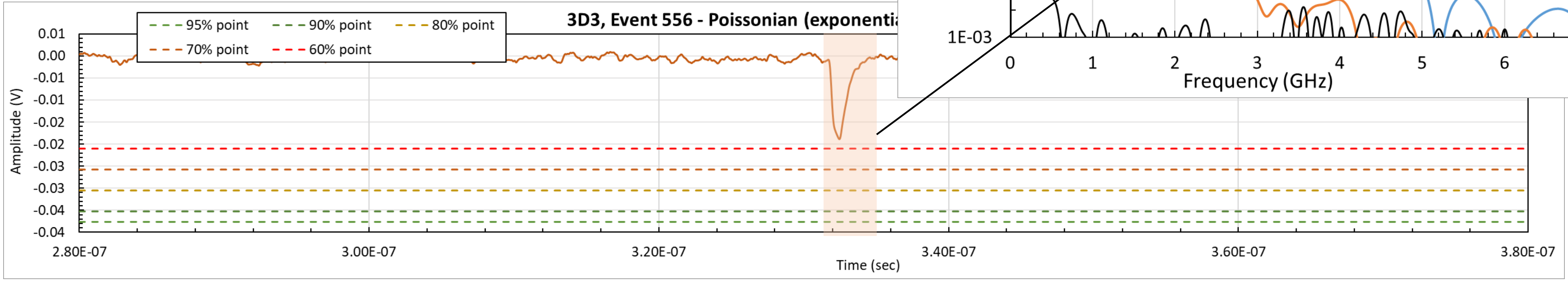

•Single Event Burn-out

Single Event Burn-Out was also observed in 3D sensors but in much higher fields with respect to LGADs (~ 25 V / μm) and on the 1e16 fluence but not 1e17

Geometry

- Charge generation and charge drift directions not parallel, **very high angles**
  - → Drifting charges do not add up to the avalanche created at the ceed point
- Much smaller capacitance (20-80 fF), smaller stored energy in the sensor to be released once conductive channel forms → Recoverable Breakdown

Irradiation

- Effect observed when concertation of defects high enough statistically

BUT

- **Carrier lifetime (trapping) should be sufficient to allow for the avalanche to evolve**

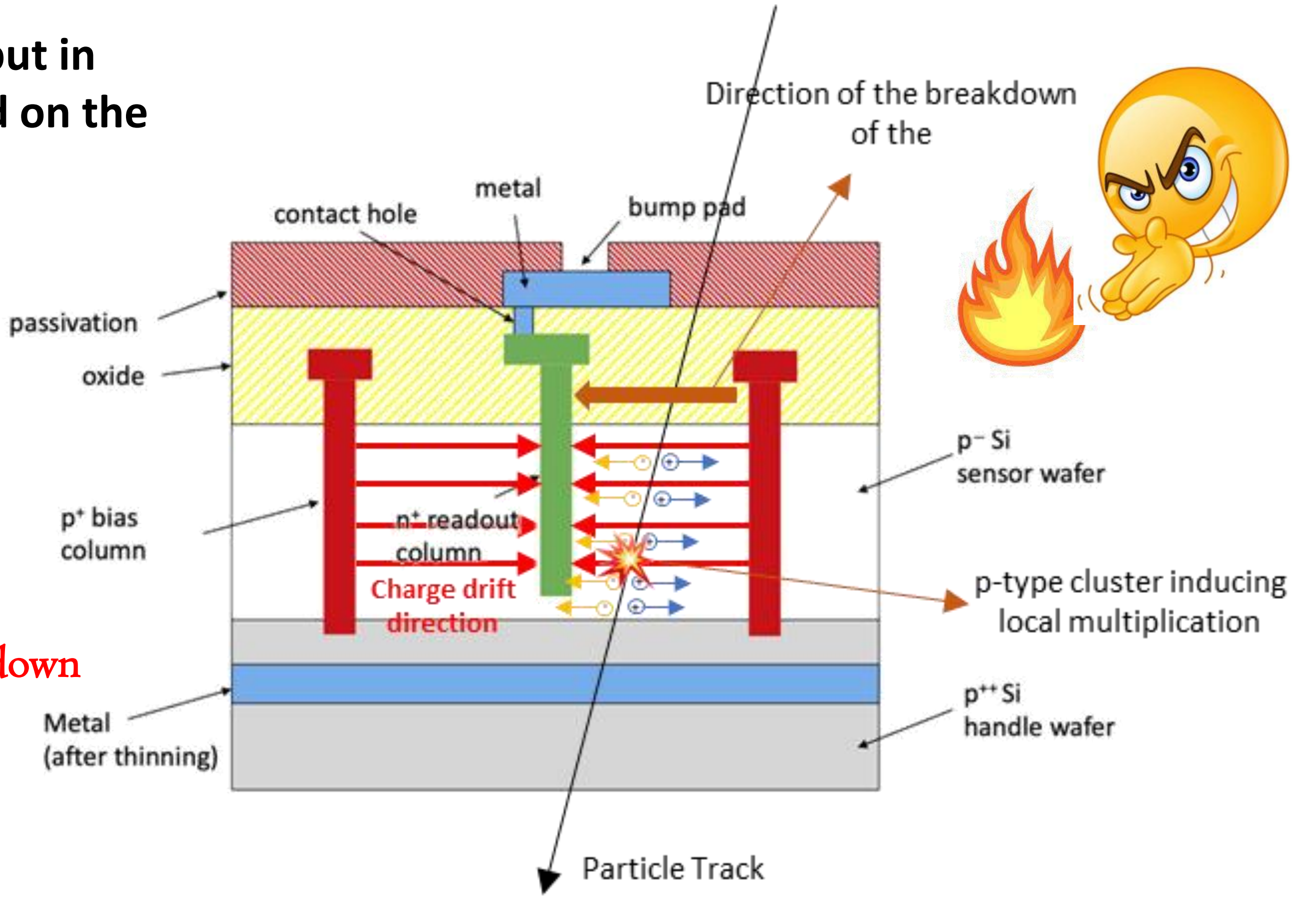

Perfect storm

- LGADs → ~ 1e15
- 3Ds → ~ 1e16

V. Gkougkousis, "LGAD Safety and Stability Concerns" – HGTD Sensor Meeting April 2018
CERN-OPEN-2023-017

•16 Channel Board

The issue….

50x50 μm², 1E

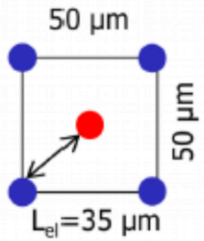

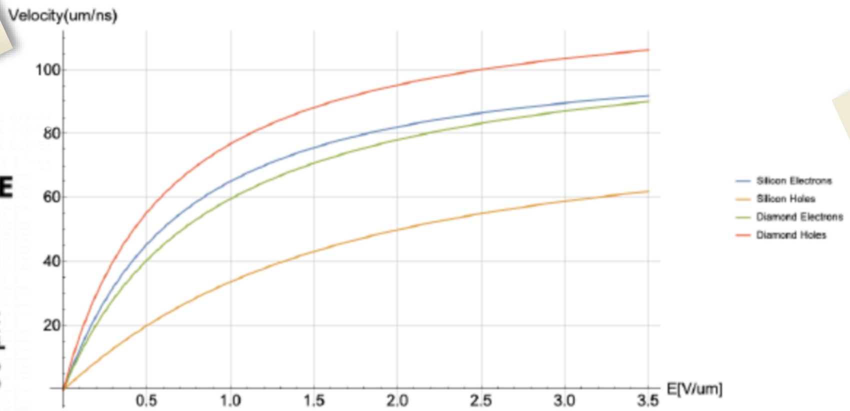

- Assuming a linear filed dependence and a -15 V operation point at 35 μm column distance:
$$|E| \cong 0.43\ V/\mu m$$
- Estimating drift velocity for electrons:
$$v^e_{drift} = \frac{\mu_{0,e} \times E}{\left[1 + \left(\frac{\mu_{0,e} \times E}{v^e_{sat.}}\right)^{\beta_e}\right]^{1/\beta_e}}$$
with $v^e_{sat.} = 107\ \mu m/ns,\ \mu_{0,e} = 1417 \frac{cm^2}{Vs},\ \beta_e = 1.109$
$$\boldsymbol{v^e_{drift} \approx 41.4\ \mu m/ns}$$
- Extrapolated Rise time and Frequency:
$$t_{Rise} \approx \frac{1}{3} \times t_s = \frac{1}{3} \times \frac{d/2}{v^e_{drift}} \approx 140\ psec \Rightarrow \mathbf{2.3\ GHz}$$

The solution

Timeline

July 2021	October 2021	April 2022	June 2023
Design submission	Initial tests	2nd Mezzanine iteration	Test beam measurement with planar matrix

- ❖ High frequency multichannel versatile board
- ❖ Mezzanine design for fast sensor interchangeability
- ❖ Suitable for matrices (AC-LGAD applications) but also for single pad devices

- ➢ High Frequency SiGe discreate electronics @ 12 GHz bandwidth
- ➢ 2 Stage configuration with a transimpedance followed by a voltage stage
- ➢ Low max current (~10mA) with well behaved gain linearity vs V_{DD}
- ➢ Ruggers 3000 High Frequency substrate
- ➢ Pre-assembled miniaturized coaxial edge connectors with panel-mounted SMA plugs (1m cable length)
- ➢ 140 x140 mm outer dimensions

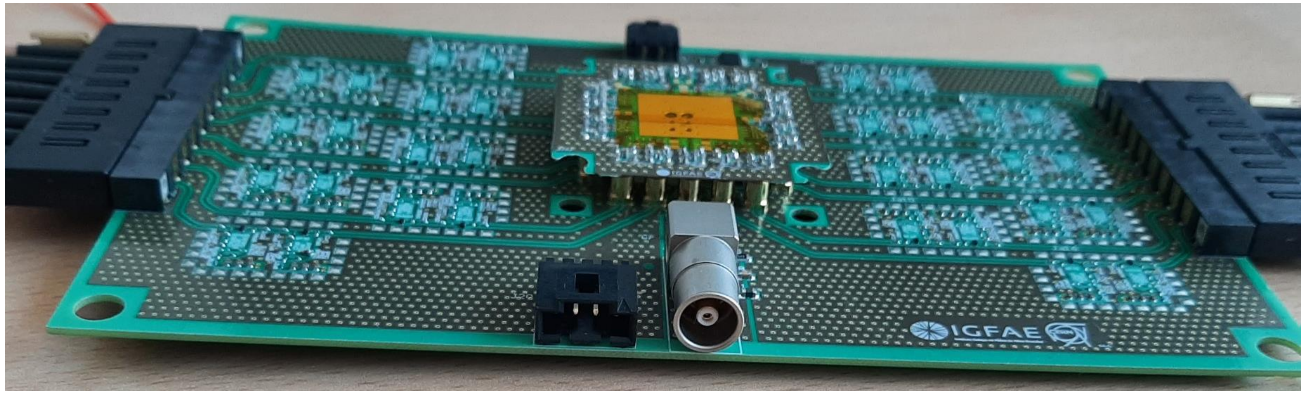

•Simulations and performance I

Initial design

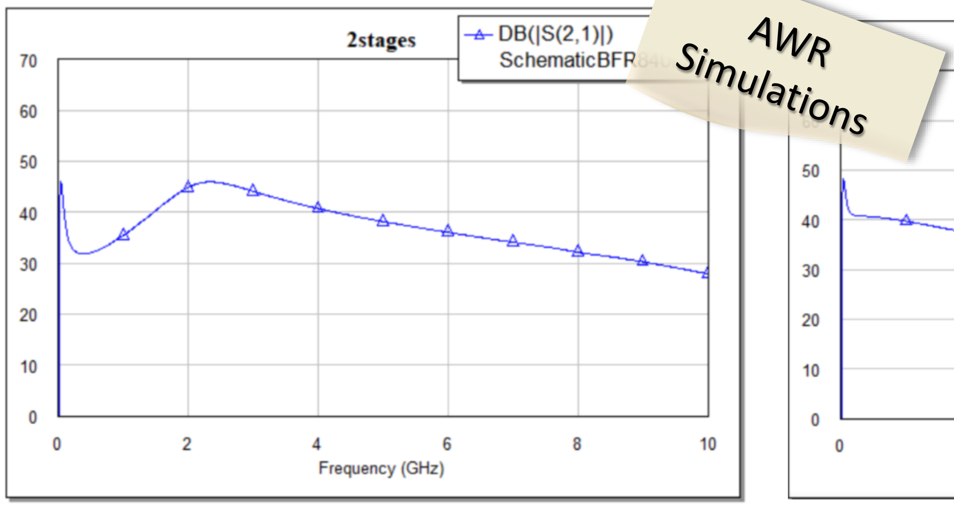

Modified –Uniform design

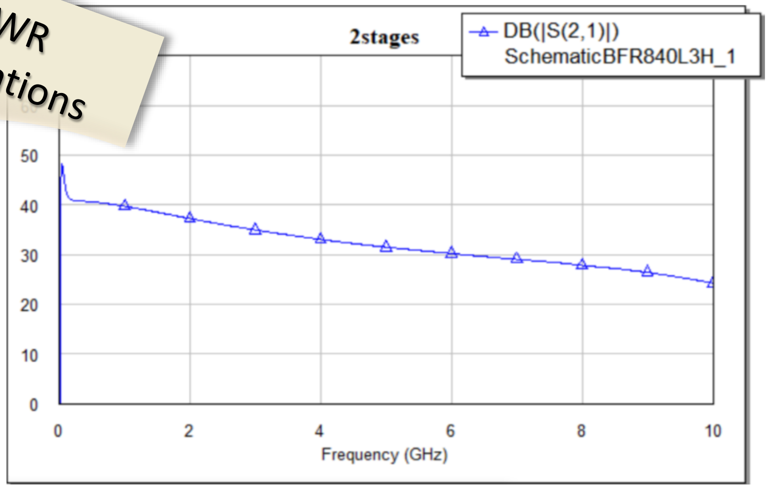

- Optimized design for uniform response with frequency
- No sharp gain change discontinuities
- No undershoot/overshoot observed
- Gain moderated to ~70 for a two-stage configuration
- 20% Higher SNR than UCSC board (with both stages)
- 2 x SNR with respect to UCSC board + niniCircuits second stage amplifier
- On going energy and transimpedance simulation

With signal injection

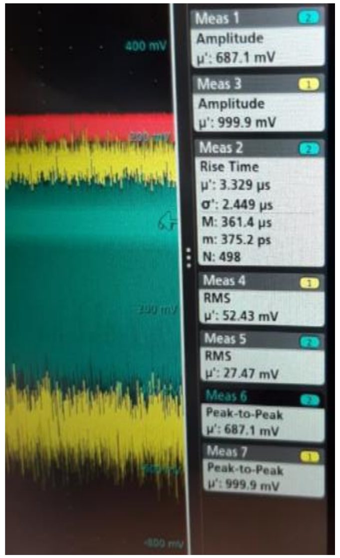

Without signal injection

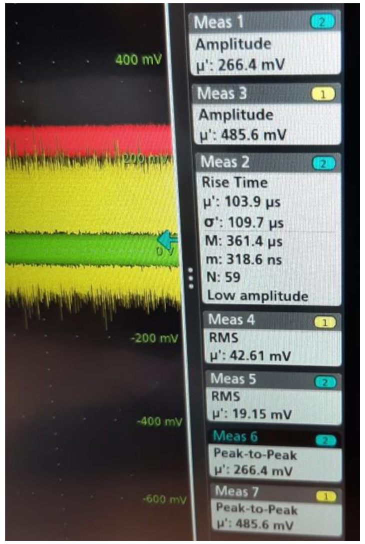

Blue: 16 channel board

Yellow: UCSC board (only one stage)

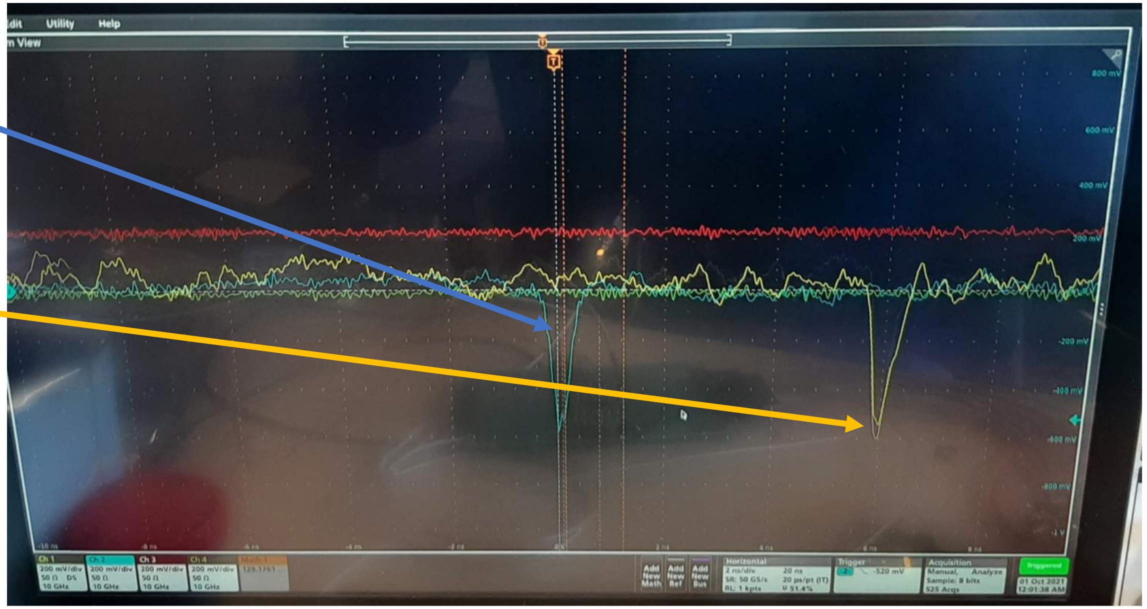

•Simulations and performance II

Edgar Lemos Cid , 18th Trento Workshop on Advanced Silicon Radiation Detectors
"Multichannel board for picosecond timing measurements of silicon sensors"

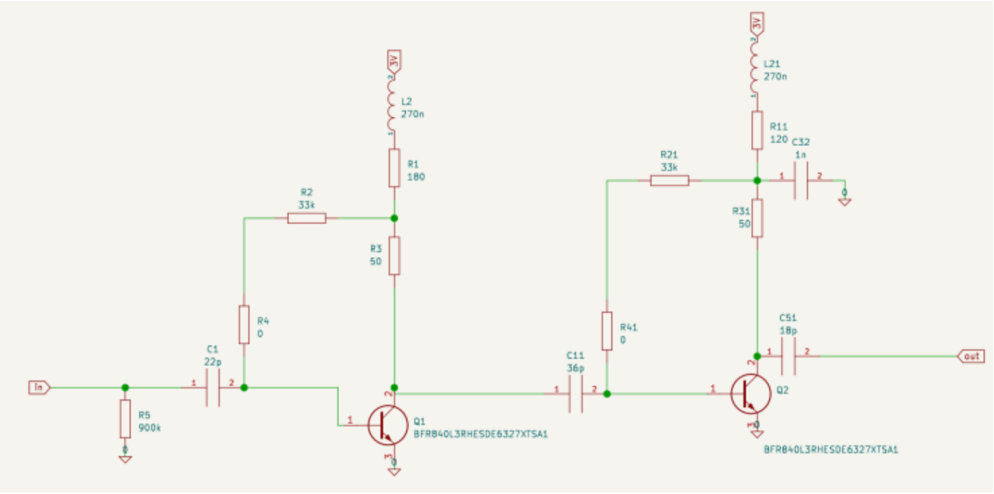

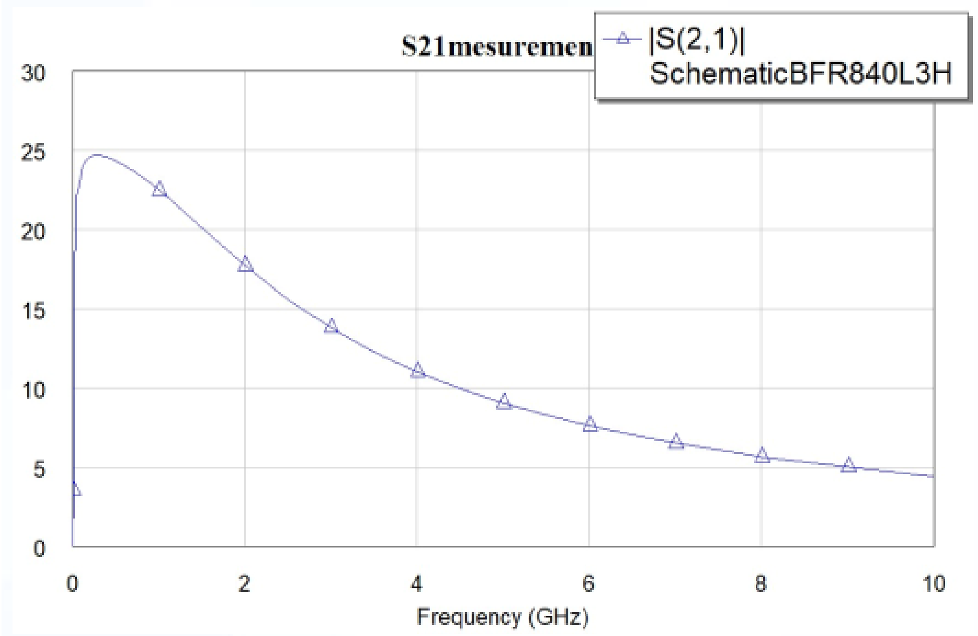

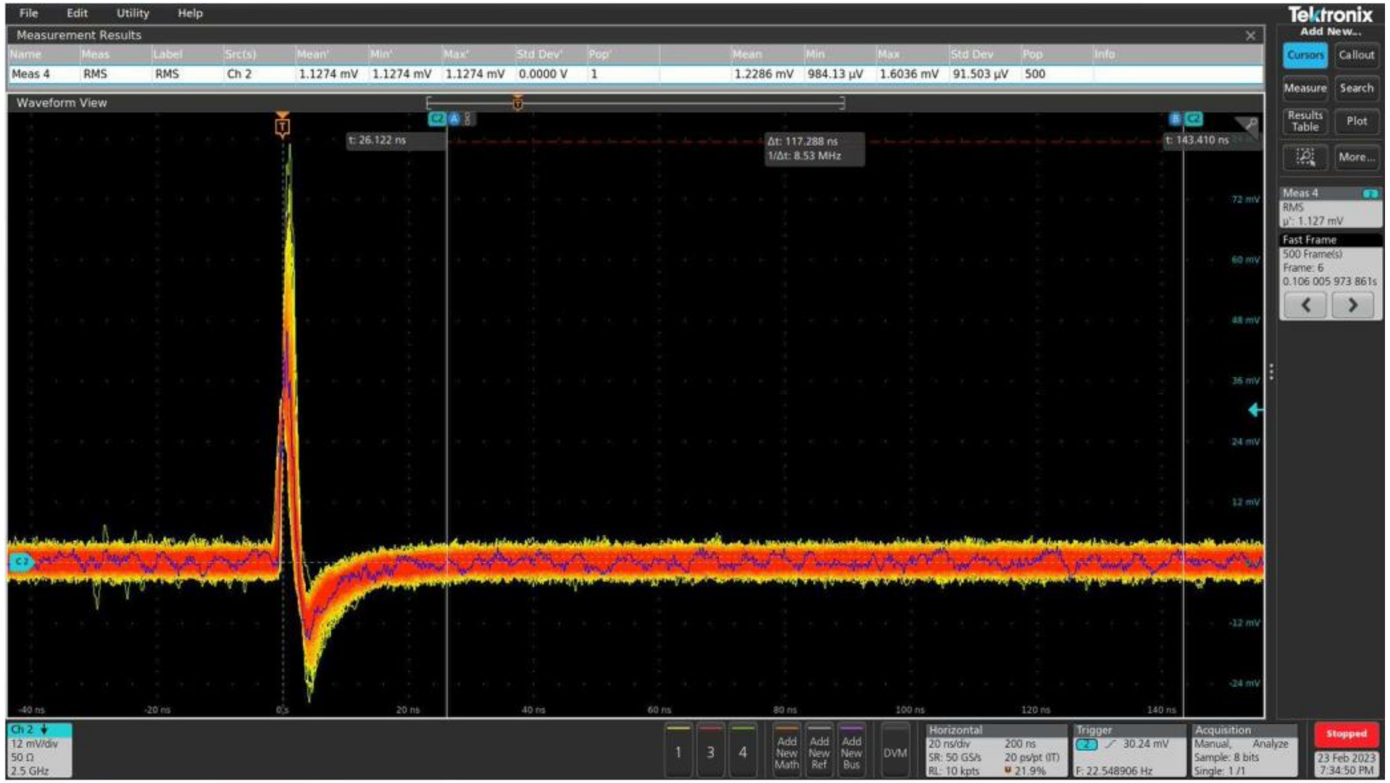

- Mean noise (~RMS) of 1.2 mV for a gain of ~ 70
- Tested with a 55 x 55 μm 3D double sided sensor of 230 μm
- Not frequency optimized for this sensor geometry with fast dropout at lower scale
- Leads to bipolar signal due to the increased trans-impedance at lower frequencies

•Conclusions

3D Pixels - Planar measurement campaign

- Several productions under investigation of different pixel size and thickness
- ***Estimate filed non-uniformity impact on time resolution vs pixel size***
- ***Determine minimal acceptable thickness for time resolution applications (SNR)***
- ***Investigate effects after irradiation up to 1e17 n_{eq}/cm^2 in protons and neutrons***

} **Primary Goals**

Test-Beam Setup

- ***Trigger Interface board:*** Versatile, allows interfacing any acquisition instrument with EUDET
- ***Control Software:*** Polymorphic UI with seeming-less multi-instrument support
- ***Cooling:*** XPS cold box with web interface temperature controllable system @ -18°C
- ***Mechanics:*** Micrometric alignment with individual DUT stages
- ***Analysis Framework:*** Advanced framework with signal shapes, iterative re-fitting and shape-based noise rejection

•Special Thanks to all the students who participated

2022 Test beam Periods

Jakob Haimberger (CERN, TU Wien)

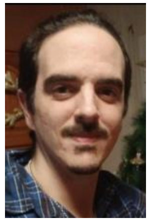

Oscar Ferrer (CNM Barcelona**)**

Hanae Tilquin (Imperial College London)

Efren Rodriguez (IGFAE)

Eloi Pazos Rial (CERN)

Alexandros Athanasios Kapelios (CERN, Uni Glasgow)

2021 Test beam Periods

Efren Rodriguez (IGFAE)

Marius Halvorsen (CERN, Oslo University)

George Petrogiannis (IFAE Barcelona)

Pablo Fernández (IFAE Barcelona)

•Backup

• Introduction

Test Geometry

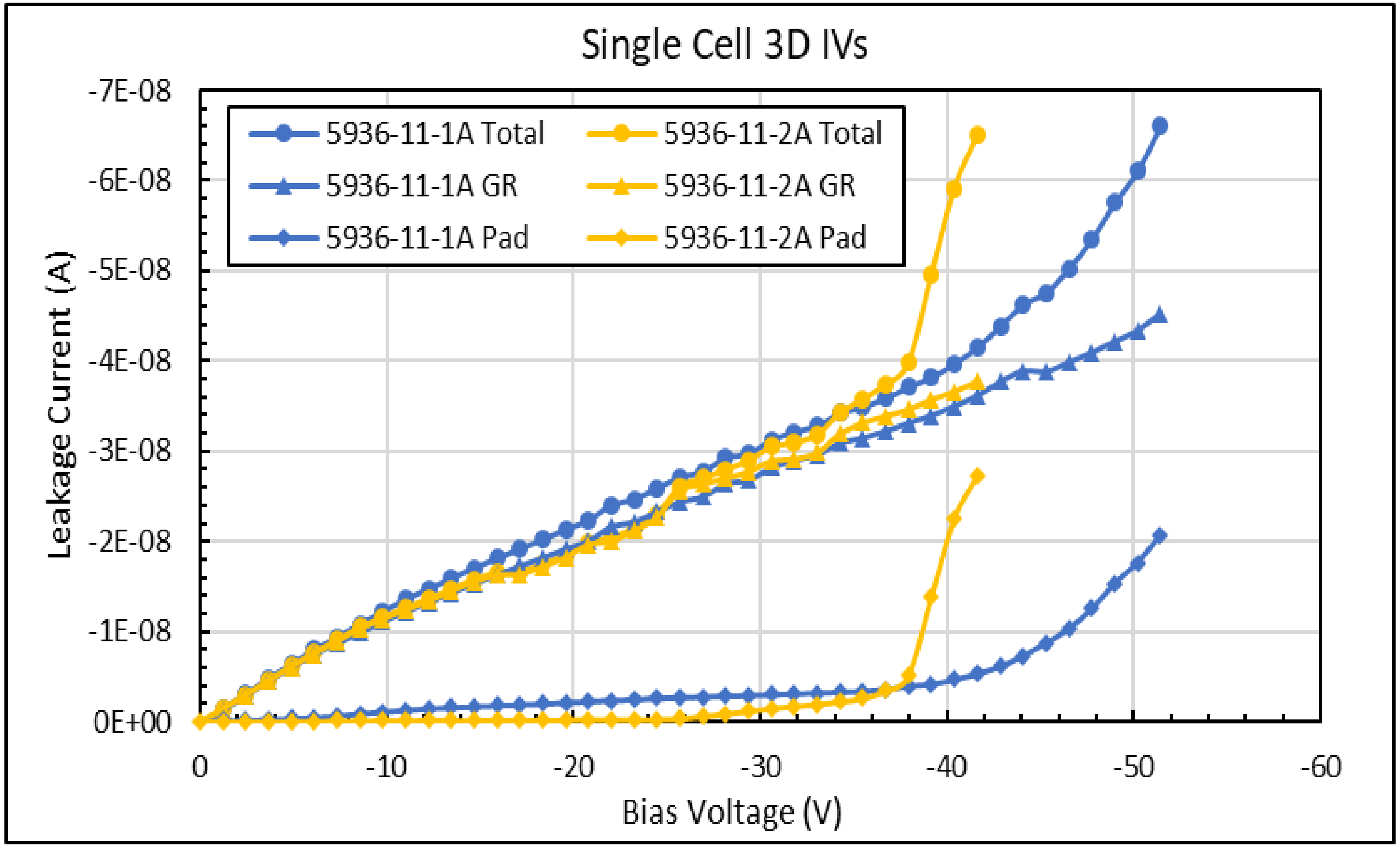

- **Compliance:** 60 uA
- **MAX Volt:** 60V
- **Voltage Step:** 1V
- **Setting time:** 2 sec
- **Averaging:** 5 measurements
- **Temperature:** 20^{o}C

• Introduction

Capacitacne

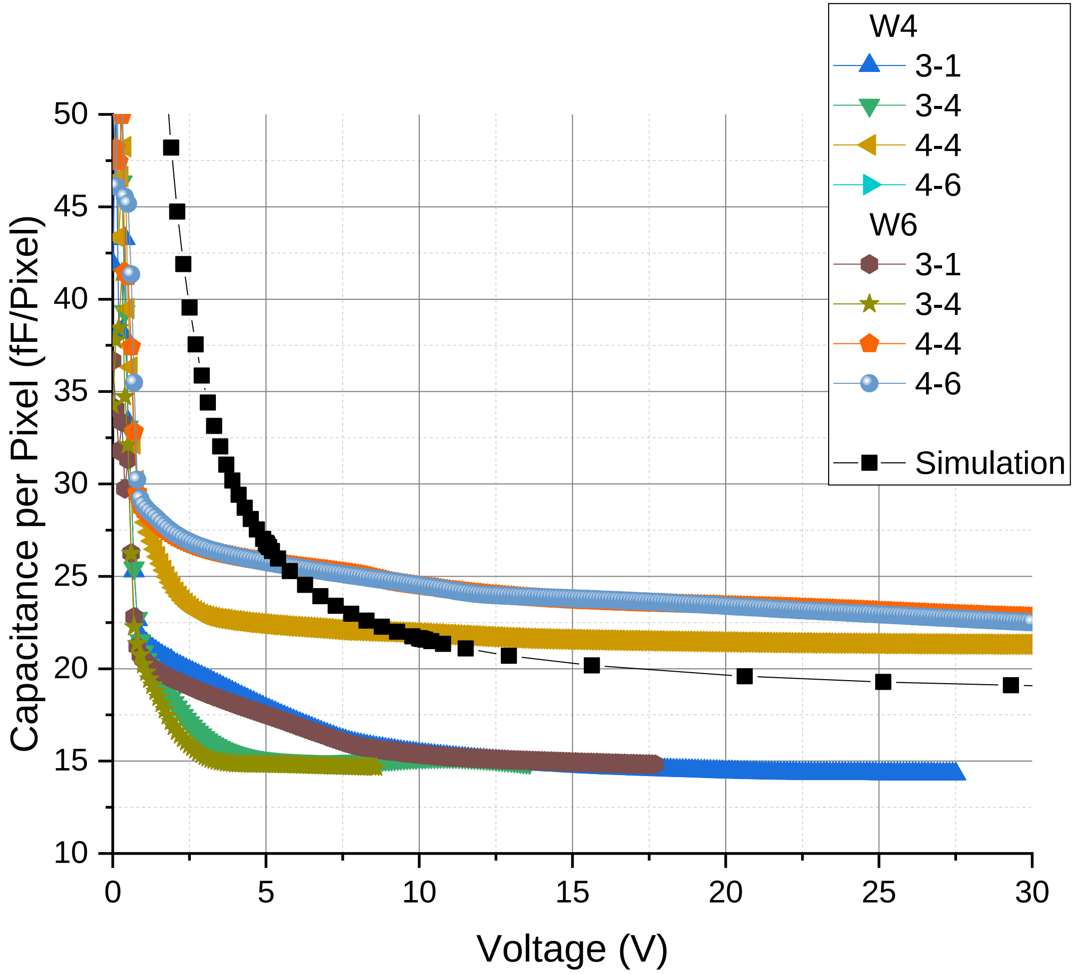

Oscar Ferrer, CNM Barcelona

Simulated pixel:

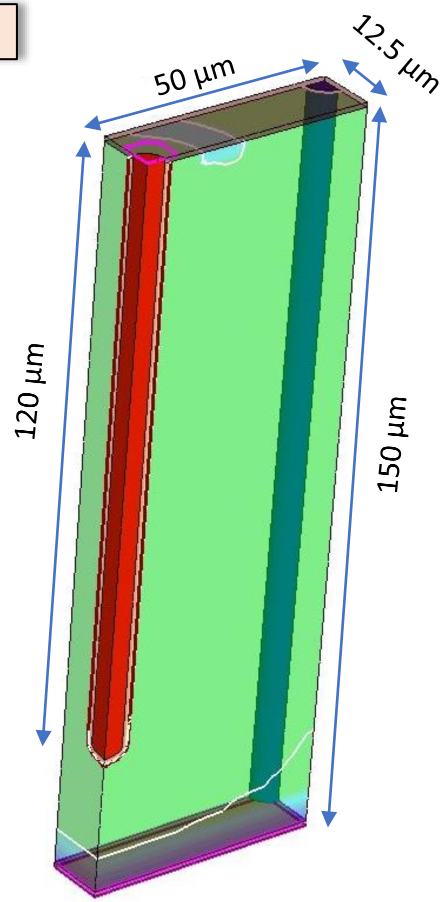

- Single-Sided
- 150µm active thickness
- 120µm deep n+ columns
- Column diameter: 8µm
- P-stop radius: 12.5µm
- ¼ column simulated → applied mirror symmetry (computational time savings)

•Signal Evolution with bias in LGADs

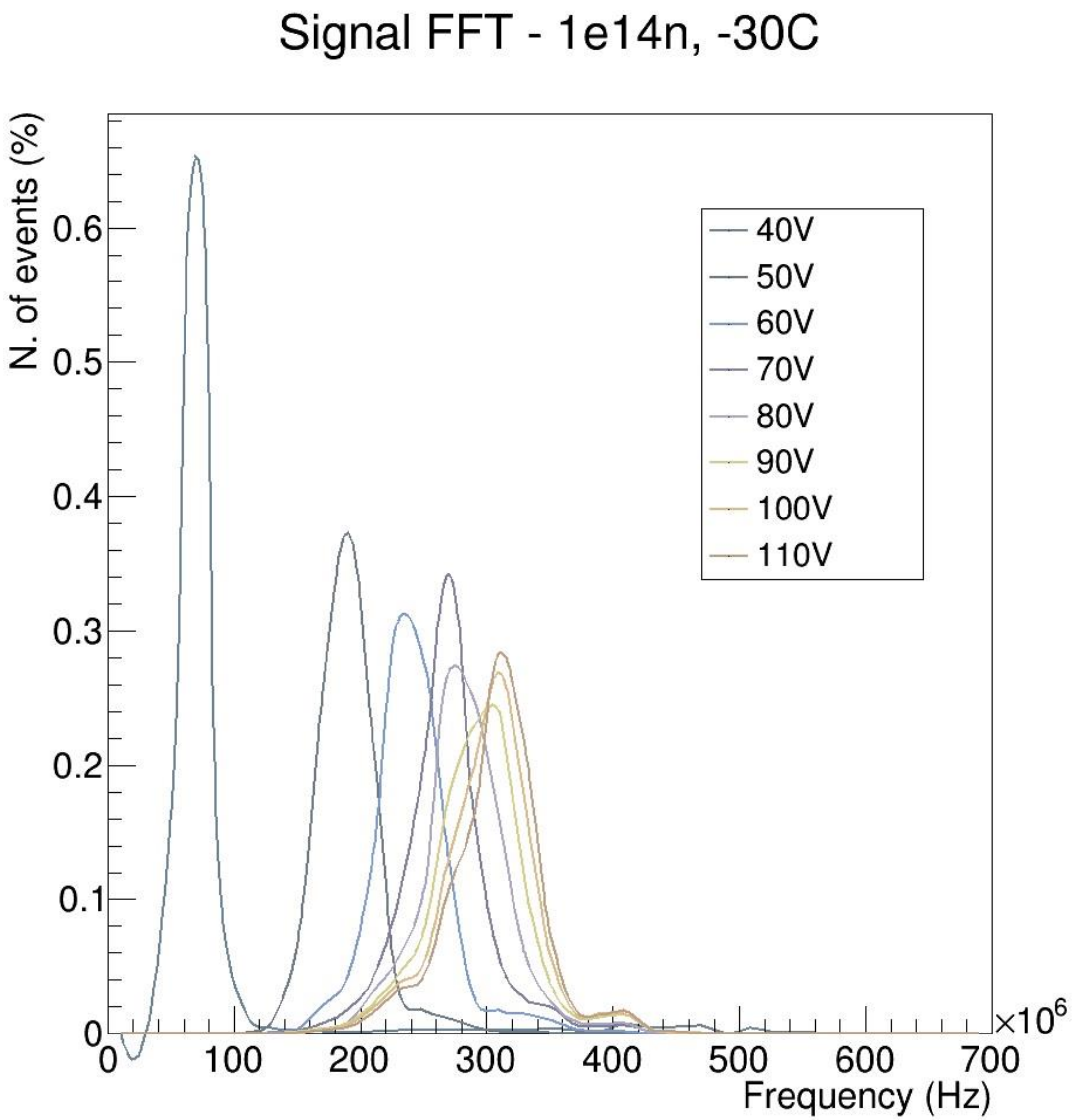

•Signal Analysis LGADs

FFT

- ✓ FFT vs Voltage presents an asymptotic behavior towards a frequency
- ✓ Asymptotic frequency depends on fluence and remaining gain
- ✓ Signal frequency increases with voltage and decreases on the onset of multiplication

Asymptotic point ~ 250 MHz

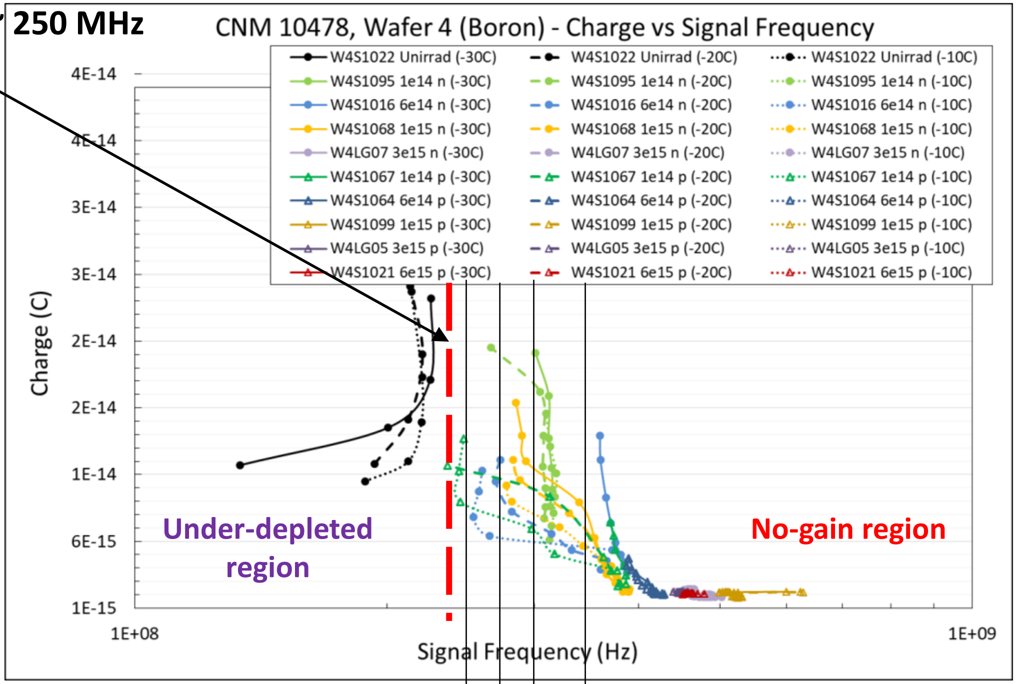

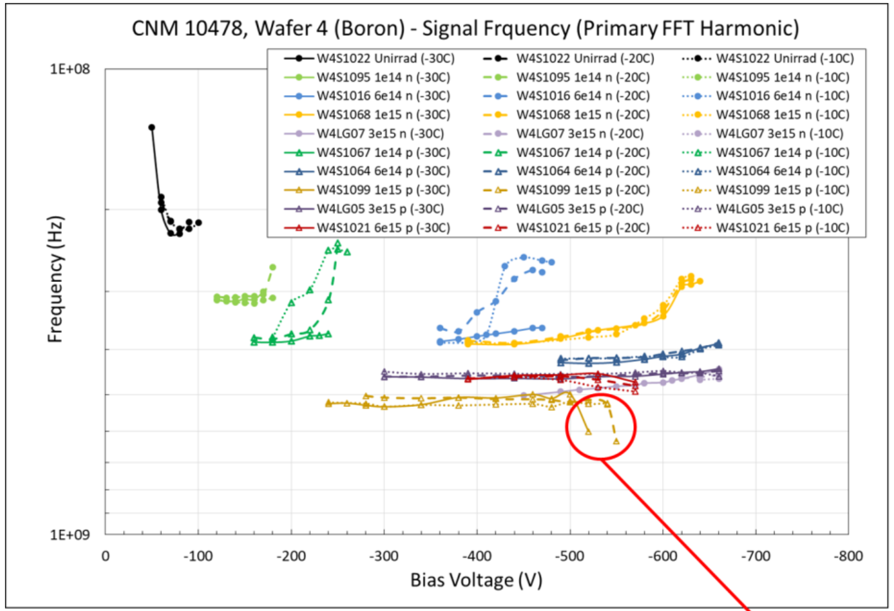

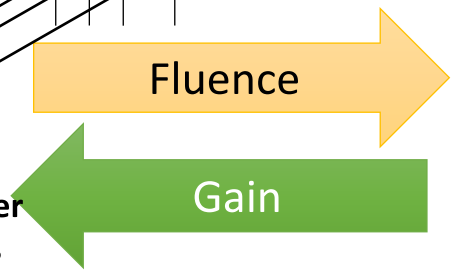

Asymptotic move to higher and higher frequencies as gain decreases and fluence increases

High Frequency noise, sensor in breakdown

•Setup @ SPS

V. Gkougkousis, 10th Beam Telescopes and Test Beams Workshop
"[Tracking the time: Single pixel 50μm pitch 3D cell time resolution map]"

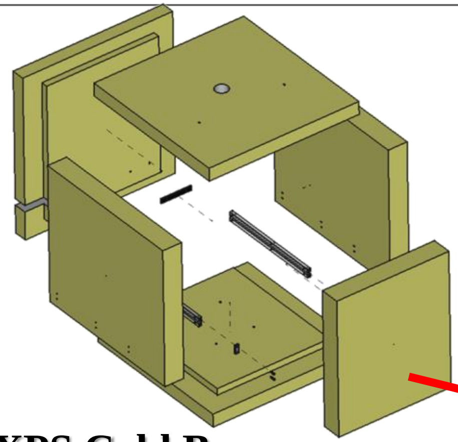

XPS Cold Box

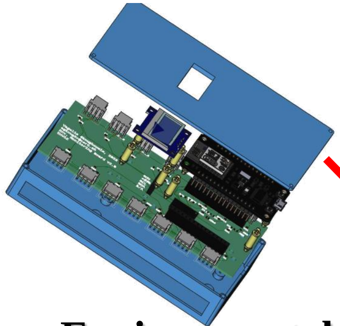

Environmental Control

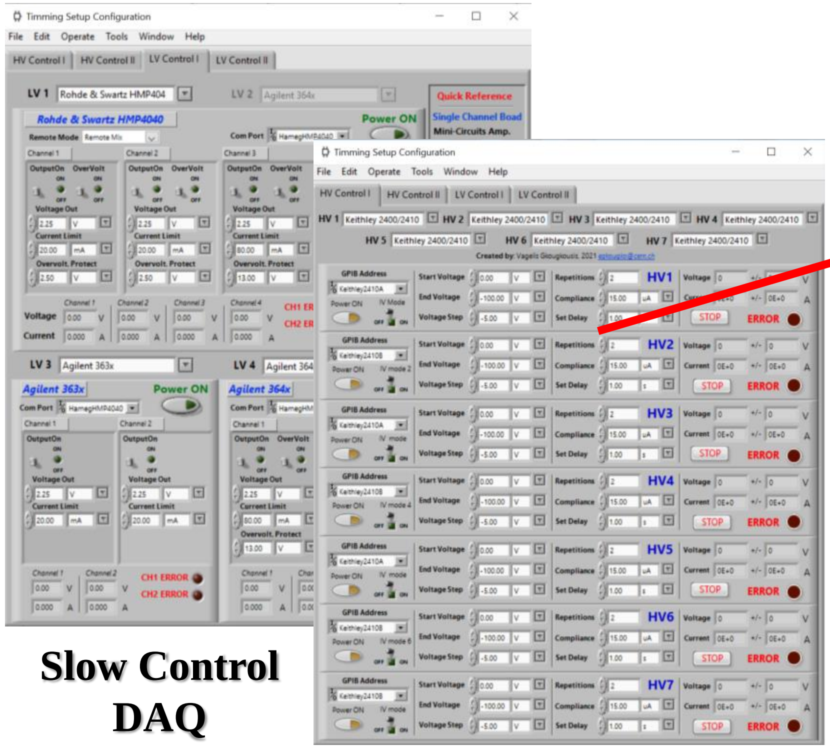

Slow Control
DAQ

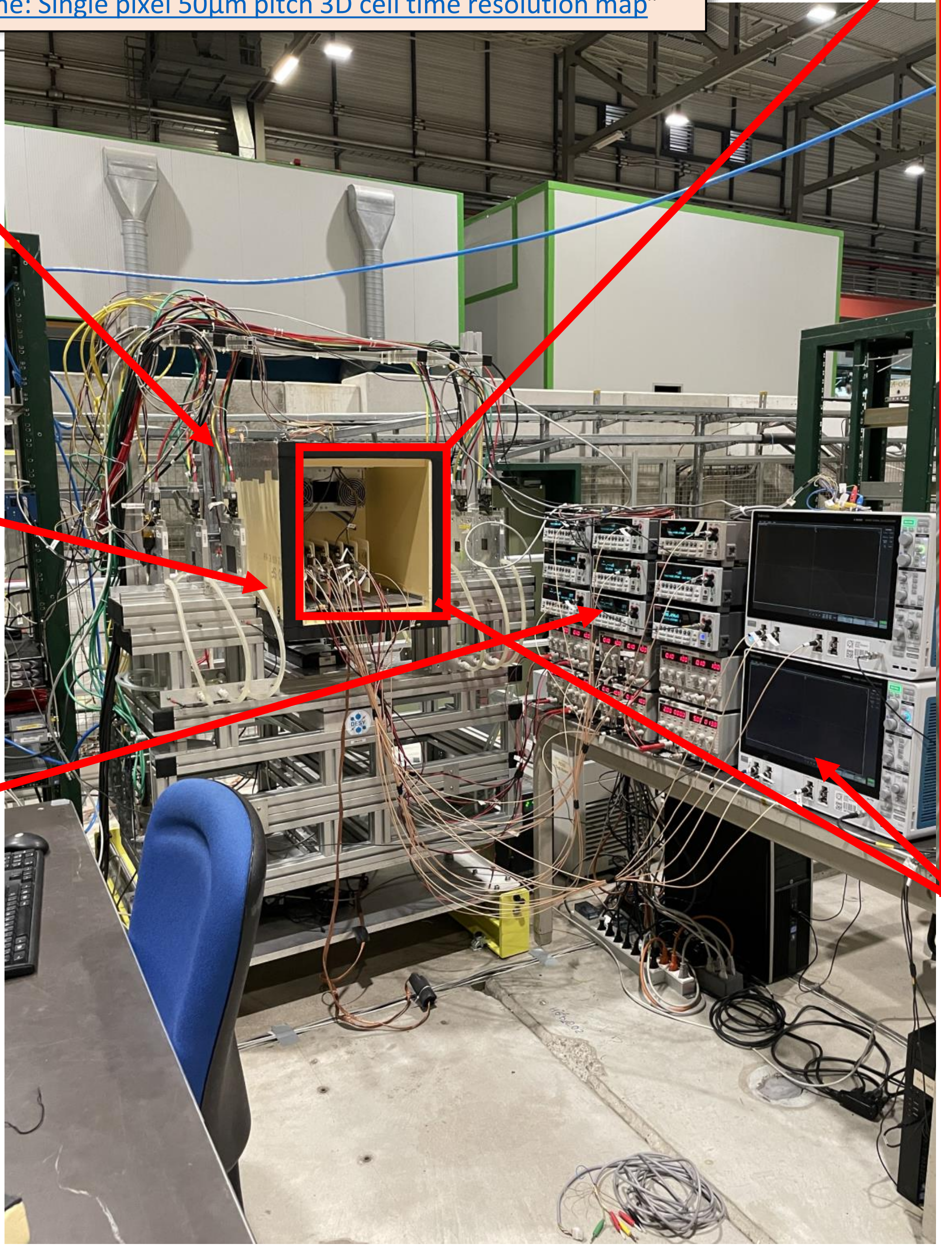

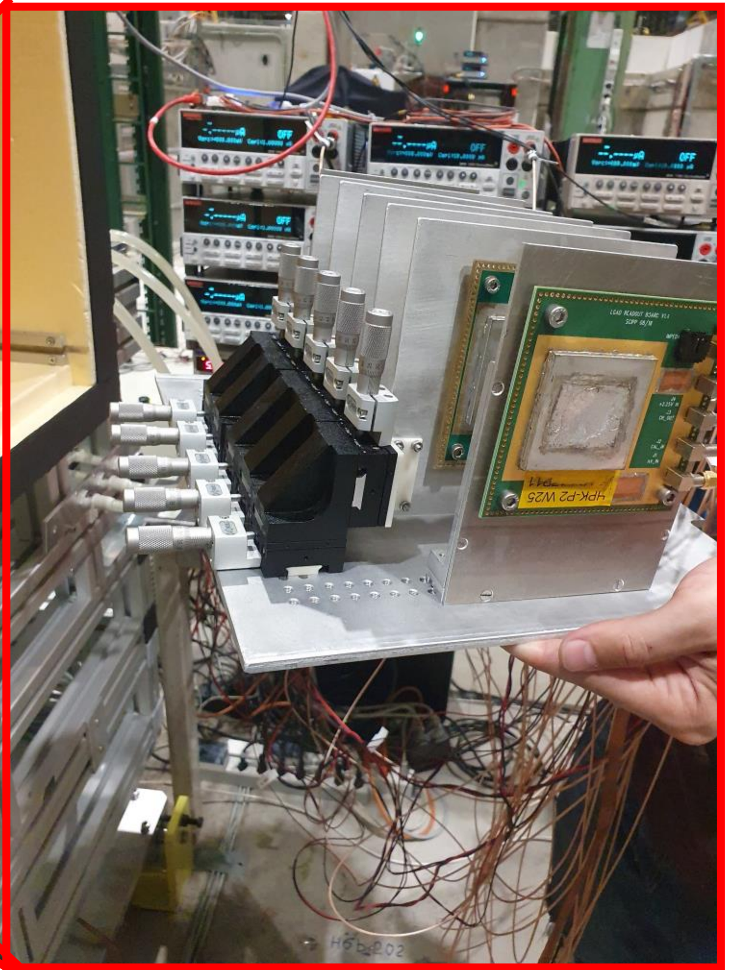

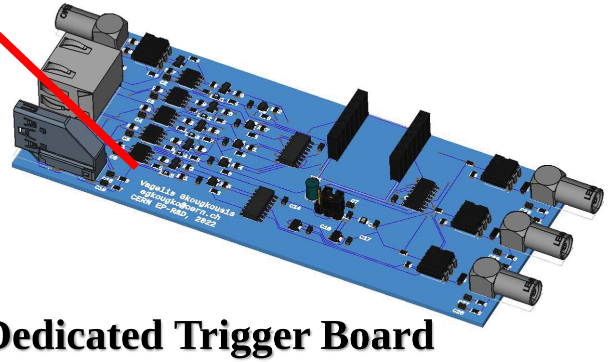

Dedicated Trigger Board

•HV & LV Control/monitoring

➢ Precompiled executable available on GitLab: here

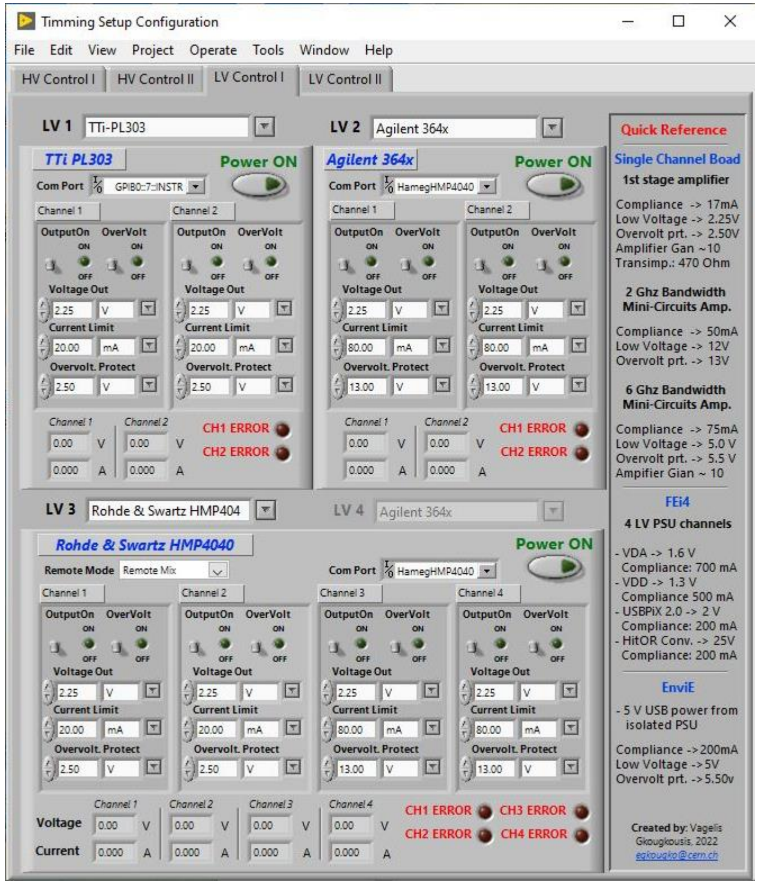

Multi-model Support with Polymorphic UI

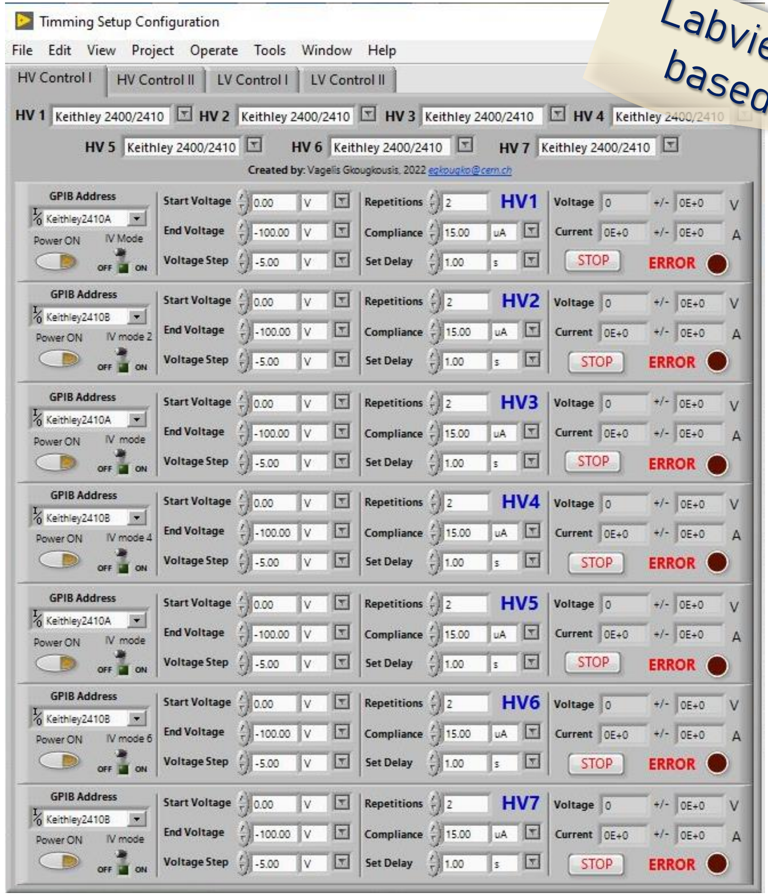

Labview based

High voltage

KEITHLEY

2400/2410 series

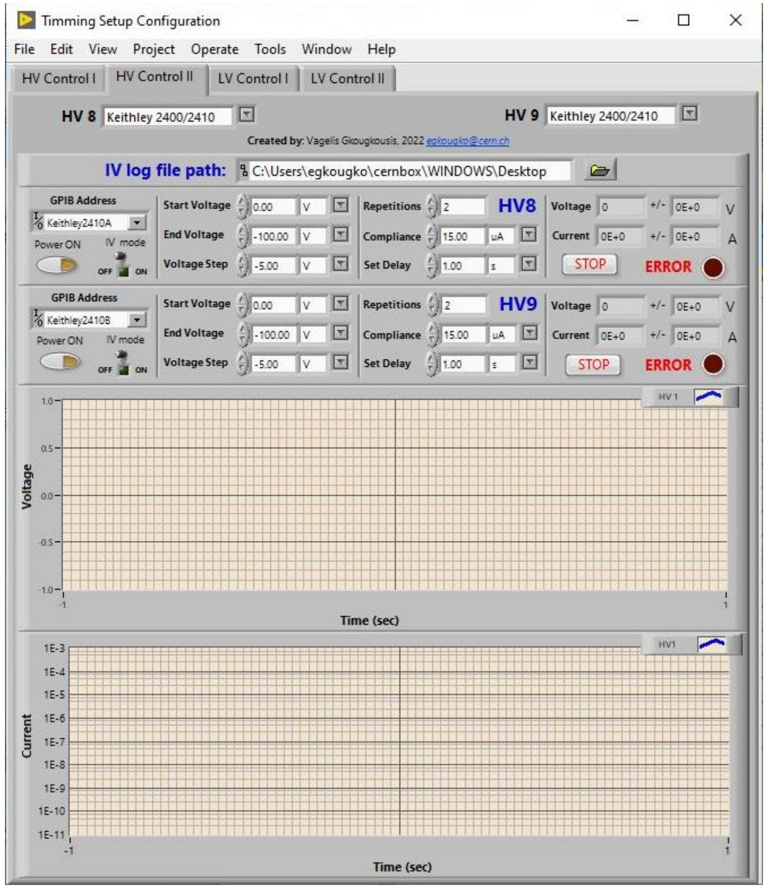

Agilent Technologies

363X series

KEYSIGHT TECHNOLOGIES

364X series

ROHDE&SCHWARZ

HMP4040

Aim TTi

PL330DP

Aim TTi

PL303QMD

- 9x HV channels
- 16x LV channels
- Constant monitoring & logging
- Live protection

•Temperature Regulation

- Running at a crisp **-18 °C**
- Glycol cooling with temperature feedback - Labview control
- Humidity regulation though N_2 feeds

- EnviE GitLab with schematics: [here]

Environmental Expander V2.0 (EnviE)

- ESP8266 based with integrated 10-bit ADC, I2C and WiFi 802.11b
- Integrated OLED 128X64 pixel screen
- High precision voltage dividers and sensor decoupling
- ARDUINO / LoUA core web interface
- Temperature resolution of 0.8 °C ± 0.06 %
- Humidity resolution 0.1 % with temperature compensation

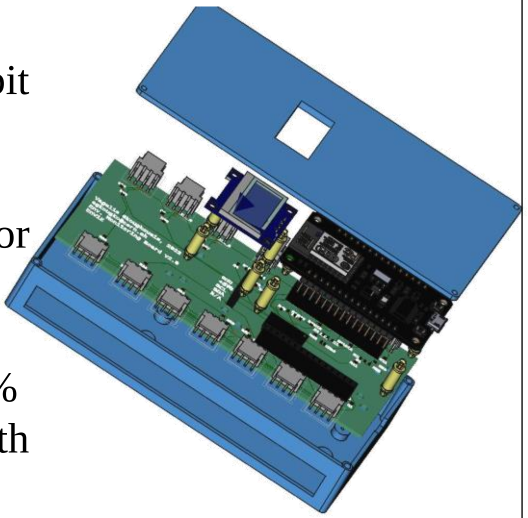

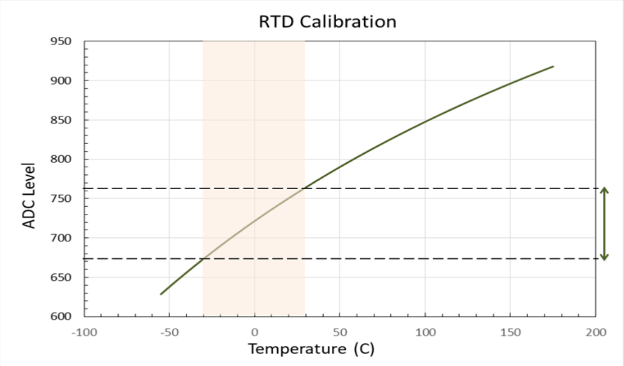

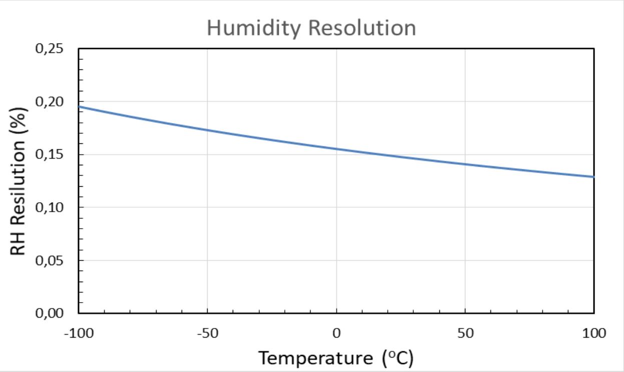

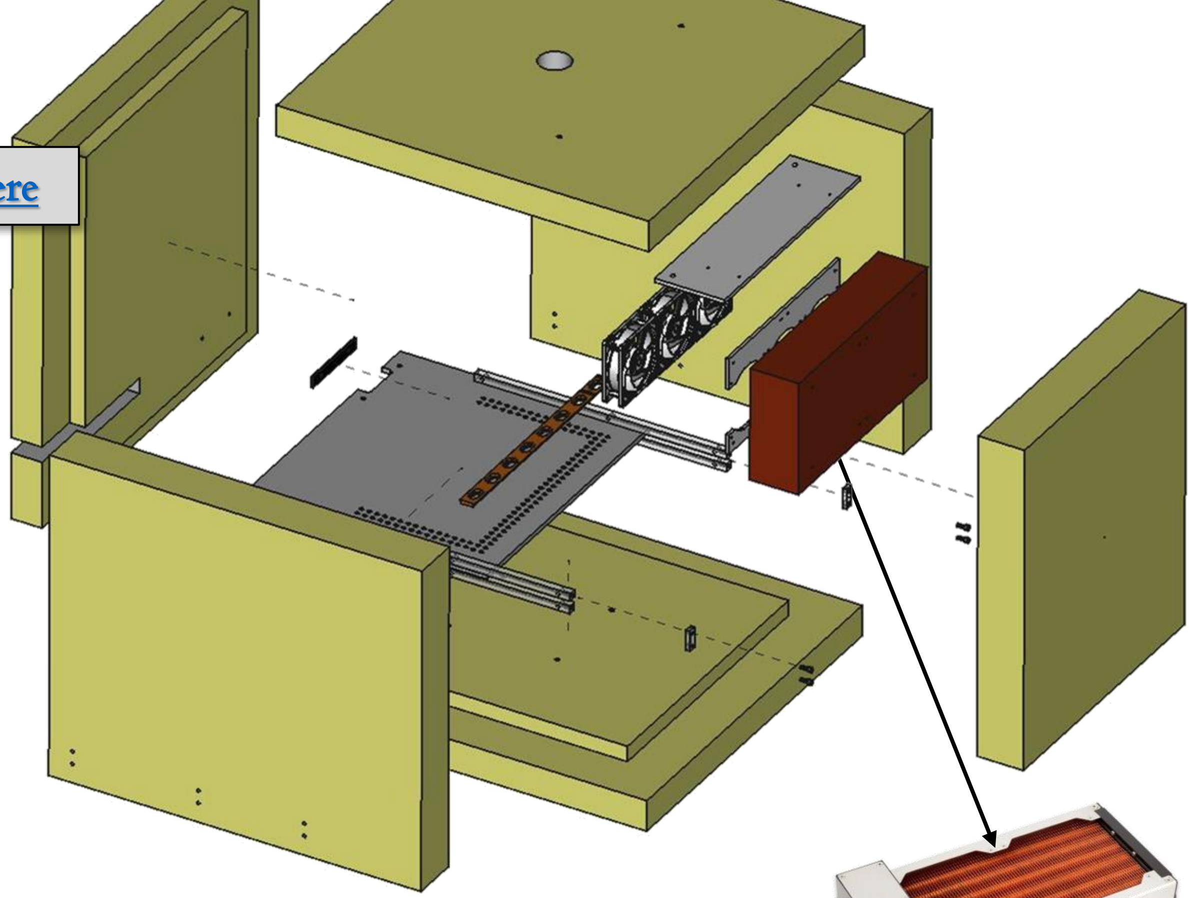

Water cooling block

- 6 c.m. thick XPS foam insulation
- Outer dimensions of 50 x 48 x 48 cm^3
- Use of commercial water-cooling block ([link])
- 3 x Axial Fan DC 80x80x25mm 24V 111.6m³/h – low remperature tested to -20°C ([link])
- Total cost ~ 400 CHF

•Readout Electronics

First Stage amplifier

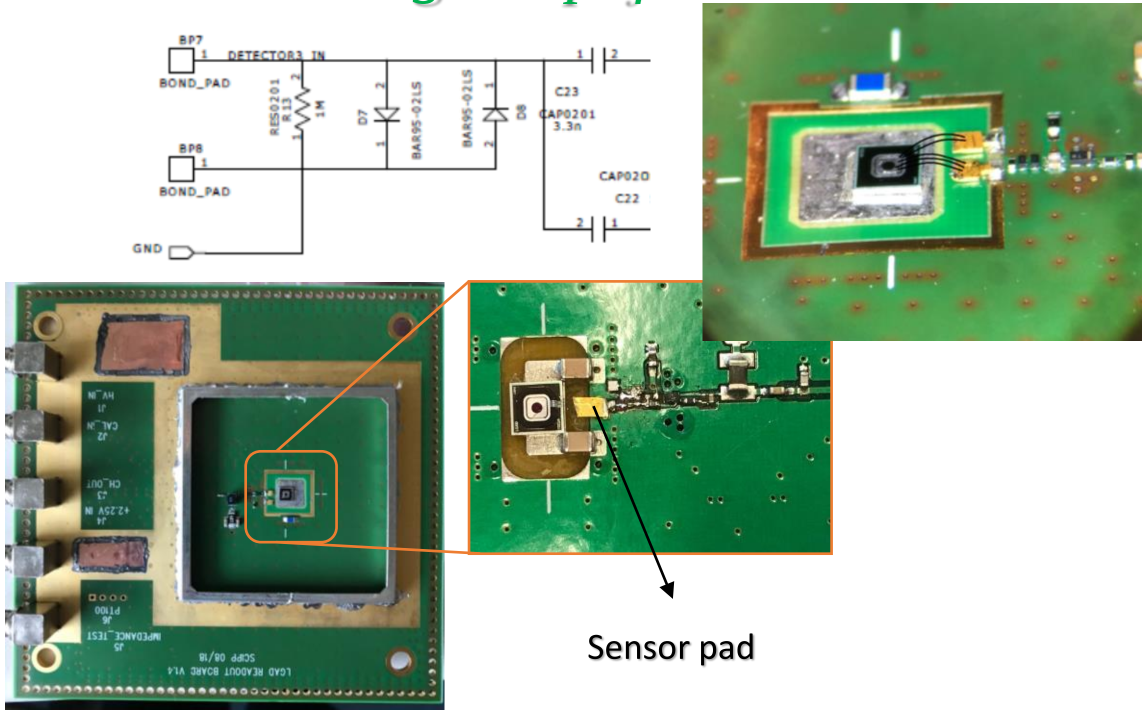

- High frequency SiGe (~12 GHz) common emitter first stage charge amplifier (470Ω trans-impedance)
- Fully enclosed faraday cage surrounding sensor
- Mean sensor + amplifier noise < 1.8 mV
- Use of identical sensors for calibration and comparison

Second Stage amplifier

- Mini-circuits (Gali 52+) Gallium arsenate voltage amplifier with a 2 GHz bandwidth for LGADs
- Mini-circuits (ZX60-V63+) 6 GHz microwave voltage amplifier for 3D and planar planes
- Amplification factor of ~ 10 at 12 and 5 V respectively
- Amplifiers mounted directly on the boards and placed inside the cold box

Gali 52+
GaAs , <2Ghz, 50Ω

ZX60-V63+
50 - 6000 MHz, 50Ω

•Analysis Framework

➢ Code available on git: https://gitlab.cern.ch/egkougko/lgadutils

➢ Four main classes with dedicated header and implementation files, one wrapper class handling user interaction

C++ 11

- LGADUtils → Wrapper to handle user I/O and pass arguments
- ➢ LGADBase → Basic framework function and infastructure
- ➢ LGADRun → Timing resolution, CFD maps, multi DUT operations
- ➢ LGADChannel → Mean pulse shape, mean pulse properties form entire run
- ➢ WaveForm → Single Waveform properties and time walk corrections
- ➢ **Bonus: LGADSel** → **Selector Class with auto-set 64 channel support**

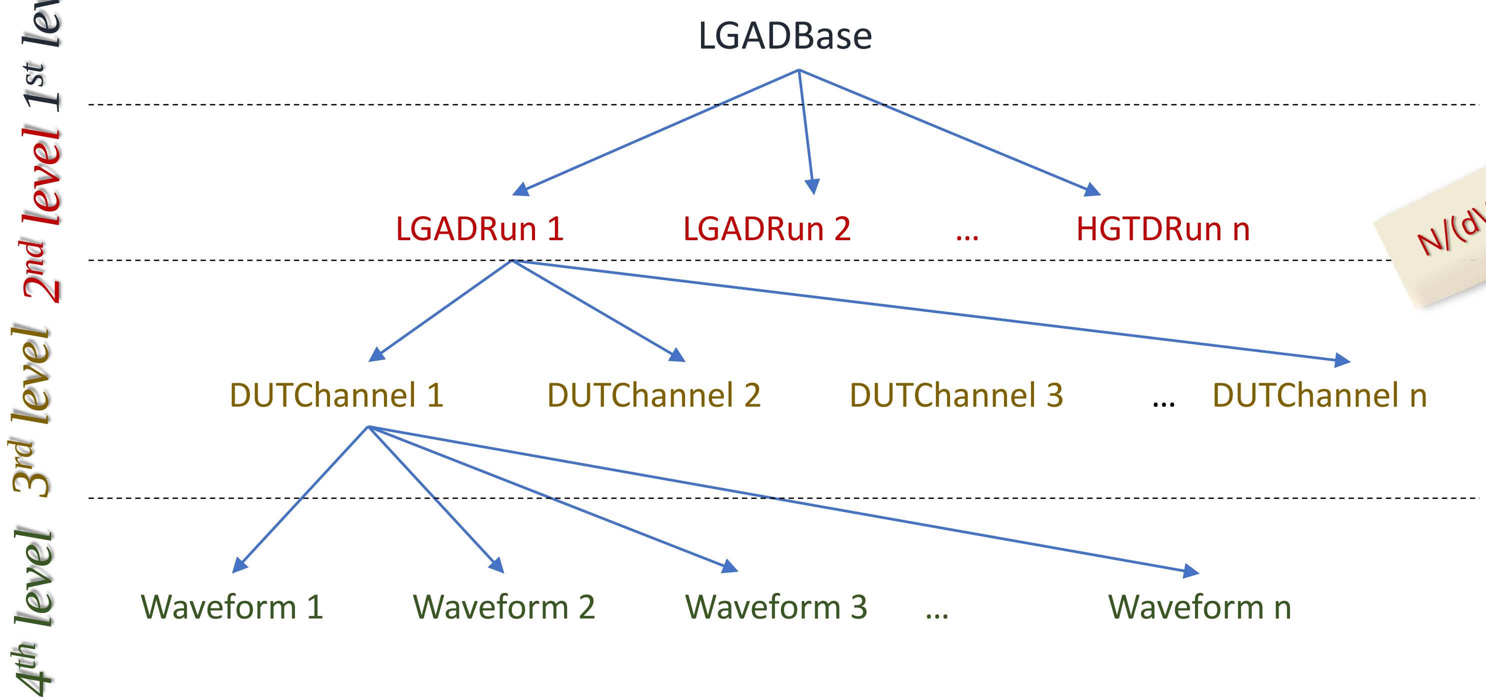

- Iterative re-fitting and re-binning algorithm
- Fitting of discrete and variable binning quantities
- Bayesian uncertainties at efficiency level
- Event by event FFT transimpedance correction

$N/(dV/dt)$, T_{Rise}/SNR

Quantity	***Applied Fit type***
Min, Max voltage :	Gauss, Gauss x Landau fit
Start, stop, min, max indices :	Gauss, Gaussian fit
Noise / pedestal :	Gaussian fit
Min, Max, Rise, Trigger time :	Gaussian fit
Charge, dV/dT, Jitter, ToT:	Gauss x Landau fit
FFT:	Variable bin Gaussian

•Event by Event Strategy

File: WaveForm.cxx

- A four sequential step analysis approach
- Analysis escalates in a pyramid structure

Five preliminary sequential steps before we even start looking at the waveform

Step 1

Set Waveform values → Determine polarity → Find max, min point → Find start, stop point → Determine if noise → Determine if pulse within window

Step 2

Define noise points → Use Gaussian fit for noise/Pedestal → Pedestal subtraction/ inversion → Recalculate start, stop points, min, max

Step 3

Compute charge → Determine rise time → Determine CFD Time → Compute dV/dT → Determine Trigger Time → Estimate Trigger & CFD ToT

Step 4

Perform CFD time to voltage Correction (Time Walk) → Signal FFT → Noise FFT

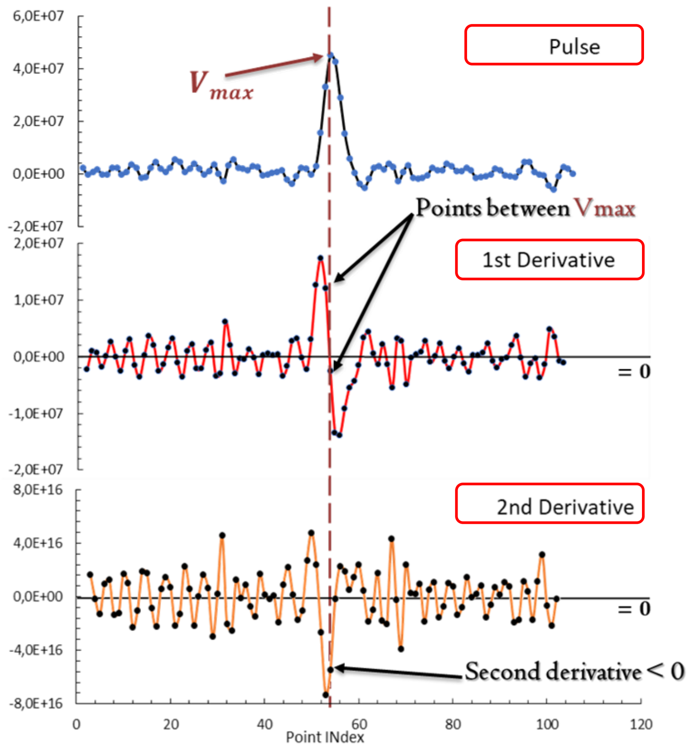

- If $SD_{maxima} > SD_{minima}$
  $D_m(max) > D_m(min)$
  or $SD_{maxima} < 1.05*SD_{minima}$
  $D_m(max) > D_m(min)$

Positive polarity

IsNoise Algorithm

Number of points with $0.8 \cdot V_{max}$

- If $N_{points} > 2$ test 0.7 , 0.6 & $0.5 \cdot V_{max}$ to account for wavy waveforms
- If $N_{points} > 2$ then require $dN_{points} < 8/12/16/20$

•Iterative Re-fitter & signal templates

File: LGADFits.cxx

- Centralized fitter engine for all fits
- Fully automated, including limits, method and Minuit minimization
- 36 Iterations per fit with limits and bin size variation to determine best combination
- Over-binning protection, automatic variable discreetness test
- Variable binning for FFT, frequency histograms
- Supported ROOFit, Standalone Minuit, Integral optimization or Shape

Dataset Type	Statistic Categorization	Bin Selection Criteria		
Discrete Datasets		Lower 3 bin number variations	Optimum Bin number	Higher 3 bin number variations
	$\frac{\left\|\lim_{fit} High - \lim_{fit} Low\right\|}{\sigma} < \sqrt{N_{elements}} < N_{bins\_max}$	$\left\lceil \lceil\sqrt{N_{elements}}\rceil - n \times \left\lceil \frac{\sqrt{N_{elements}} - \frac{\left\|\lim_{fit} High - \lim_{fit} Low\right\|}{\sigma}}{3} \right\rceil \right\rceil$ with 1 < n < 3	$\lceil\sqrt{N_{elements}}\rceil$	$\left\lceil \lceil\sqrt{N_{elements}}\rceil + n \times \left\lceil \frac{N_{bins\_max} - \sqrt{N_{elements}}}{3} \right\rceil \right\rceil$ with 1 < n < 3 **
		Lowest bin number	Rest of the bin number array	
	$\sqrt{N_{elements}} \leq \frac{\left\|\lim_{fit} High - \lim_{fit} Low\right\|}{\sigma} < N_{bins\_max}$	$\lfloor\sqrt{N_{elements}}\rfloor$	$\lfloor\sqrt{N_{elements}}\rfloor + n \times \left\lceil \left\|N_{bins\_max} - \sqrt{N_{elements}}\right\| / 6 \right\rceil$ with 1 < n < 6 **	
	$\sqrt{N_{elements}} \leq N_{bins\_max} < \frac{\left\|\lim_{fit} High - \lim_{fit} Low\right\|}{\sigma}$			
	$N_{bins\_max} \leq \sqrt{N_{elements}}$	$n \times \lceil N_{bins\_max} / 7 \rceil$ with 1 < n < 7		
Continuous Datasets		Lower 3 bin number variations	Optimum Bin number	Higher 3 bin number variations
	$\frac{\left\|\lim_{fit} High - \lim_{fit} Low\right\|}{\sigma} < \sqrt{N_{elements}}$	$\left\lceil \lceil\sqrt{N_{elements}}\rceil - n \times \left\lceil \frac{\sqrt{N_{elements}} - \frac{\left\|\lim_{fit} High - \lim_{fit} Low\right\|}{\sigma}}{3} \right\rceil \right\rceil$ with 1 < n < 3	$\lceil\sqrt{N_{elements}}\rceil$	$\left\lceil \lceil\sqrt{N_{elements}}\rceil + n \times \left\lceil \frac{\frac{\left\|\lim_{fit} High - \lim_{fit} Low\right\|}{\sigma}}{3} \right\rceil \right\rceil$ with 1 < n < 3
	$\sqrt{N_{elements}} \leq \frac{\left\|\lim_{fit} High - \lim_{fit} Low\right\|}{\sigma}$	$\left\lceil \left\lceil \frac{\left\|\lim_{fit} High - \lim_{fit} Low\right\|}{\sigma} \right\rceil - n \times \left\lceil \frac{\frac{\left\|\lim_{fit} High - \lim_{fit} Low\right\|}{\sigma} - \sqrt{N_{elements}}}{3} \right\rceil \right\rceil$ with 1 < n < 3	$\left\lceil \frac{\left\|\lim_{fit} High - \lim_{fit} Low\right\|}{\sigma} \right\rceil$	$\left\lceil \frac{\left\|\lim_{fit} High - \lim_{fit} Low\right\|}{\sigma} + n \times \left\lceil \frac{\sqrt{N_{elements}}}{3} \right\rceil \right\rceil$ with 1 < n < 3

Template Method

- Point by Point projection of all time-walk corrected (though CFD) signal pulses
- Landau X Gauss fit on projected point by point distribution
- Extraction of a "characteristic" signal composed of the MPVs of the Point by point projection fits
- RooKeyPdf for analytical description of signal
- Re-iteration on all events and fit of each waveform with the extrapolated analytical signal description
- Re-caclculate all quantities

•Sensor Daughterboard

Edgar Lemos Cid , 18th Trento Workshop on Advanced Silicon Radiation Detectors
“Multichannel board for picosecond timing measurements of silicon sensors”

Sensor board

- Two types of designs. (15x15 mm and 5x5 mm central pad).
- 41 x 41 mm square shape.
- Rogers 4350B for the high speed signals.
- Connector area reinforce with 0.3 μm FR4.
- Under sensor pad thickness of 100 μm.
- Multiple drills design on the central pad to place different types and sensors sizes.
- 140 boards produced at Gacem.

Back side

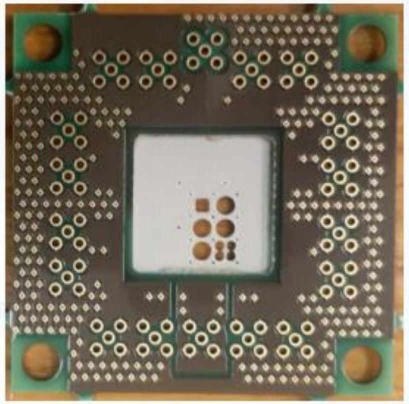

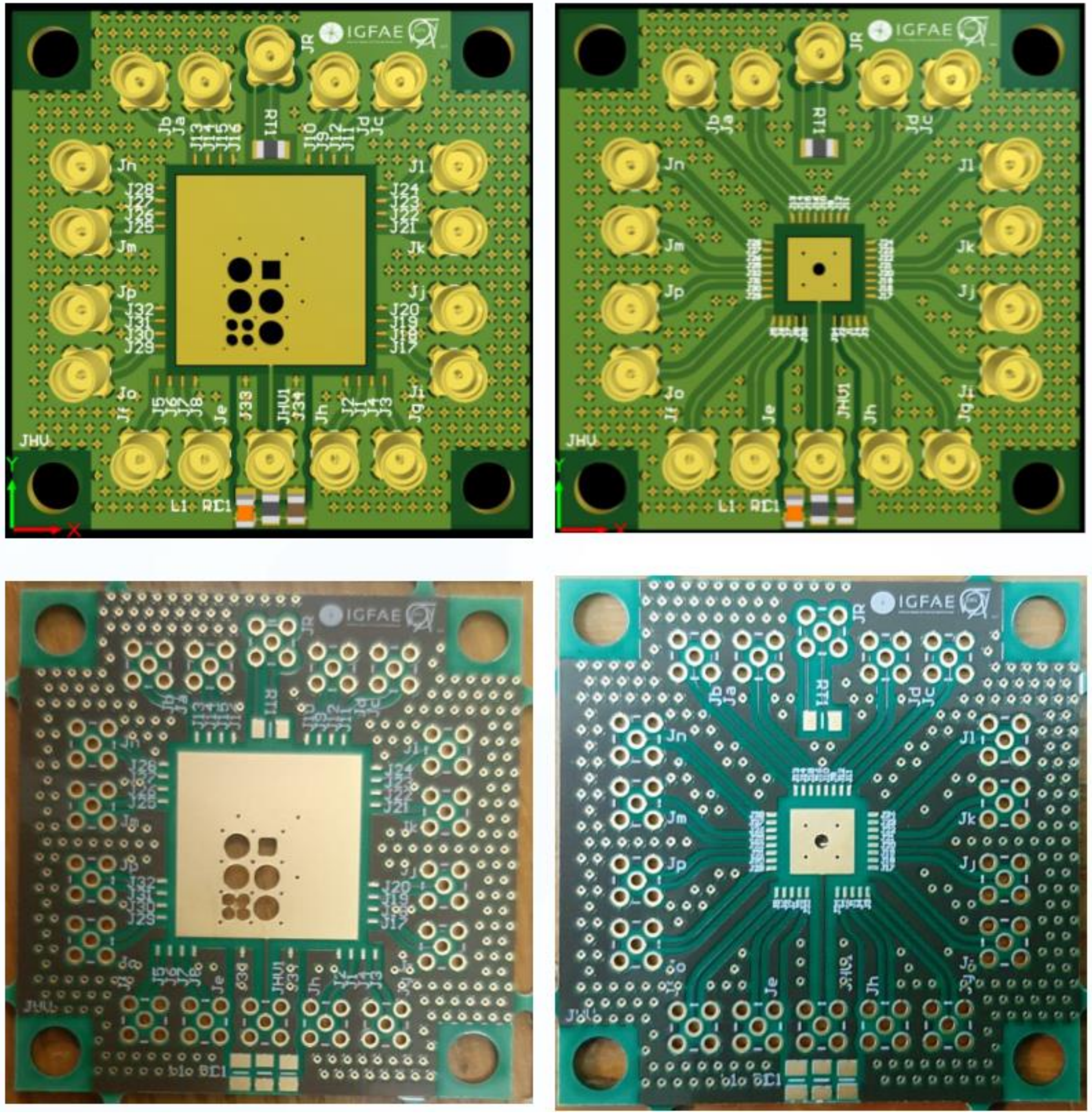

•H/W and S/W developed

Category	Function	Description	Github Project Link
Electronics	**TiB Board**	Interface and synchronize oscilloscope with AIDA TLU	Trigger Interface Board - TiB
	FEi4 HitOr Converter	Convert CMOS level output to TTL level necessary for ROI trigger	HitOr Converter
	Environmental Expander (EnviE)	Monitor Temperature / Humidity at DUT level	Environemental Monitoring Expander - EnviE
	Front-End readout board	12 GHz fast transimpedance amplifier with integrated faraday cage	Single Channel Board
Mechanics	**Cold-Box and DUT Support**	XPS foam enclosure for -20C operation and individual DUT alignment	Test beam Mechanics
Software	**Oscilloscope Fast DAQ**	SCPI layer DAQ program for oscilloscope readout	Oscilloscope DAQ
	Power/ Temp Control Software	Labview based Low Voltage and HV control software with integrated single event burnout protection	TiCAS - Timing Control Automation Software
	Trimming analysis Software	LGADUtils timing analysis framework	LGADUtils

•Single Event Burn-out

V. Gkougkousis, "LGAD Safety and Stability Concerns " – HGTD Sensor Meeting April 2018
CERN-OPEN-2023-017

Single Event Burn-Out was also observed in 3D sensors but in much Higher fields than LGADs (~ 30 V / μm) but 1e16 (not 1e17)

BUT

Sensors don't need to operate at that region, efficient at lower fields

Geometry

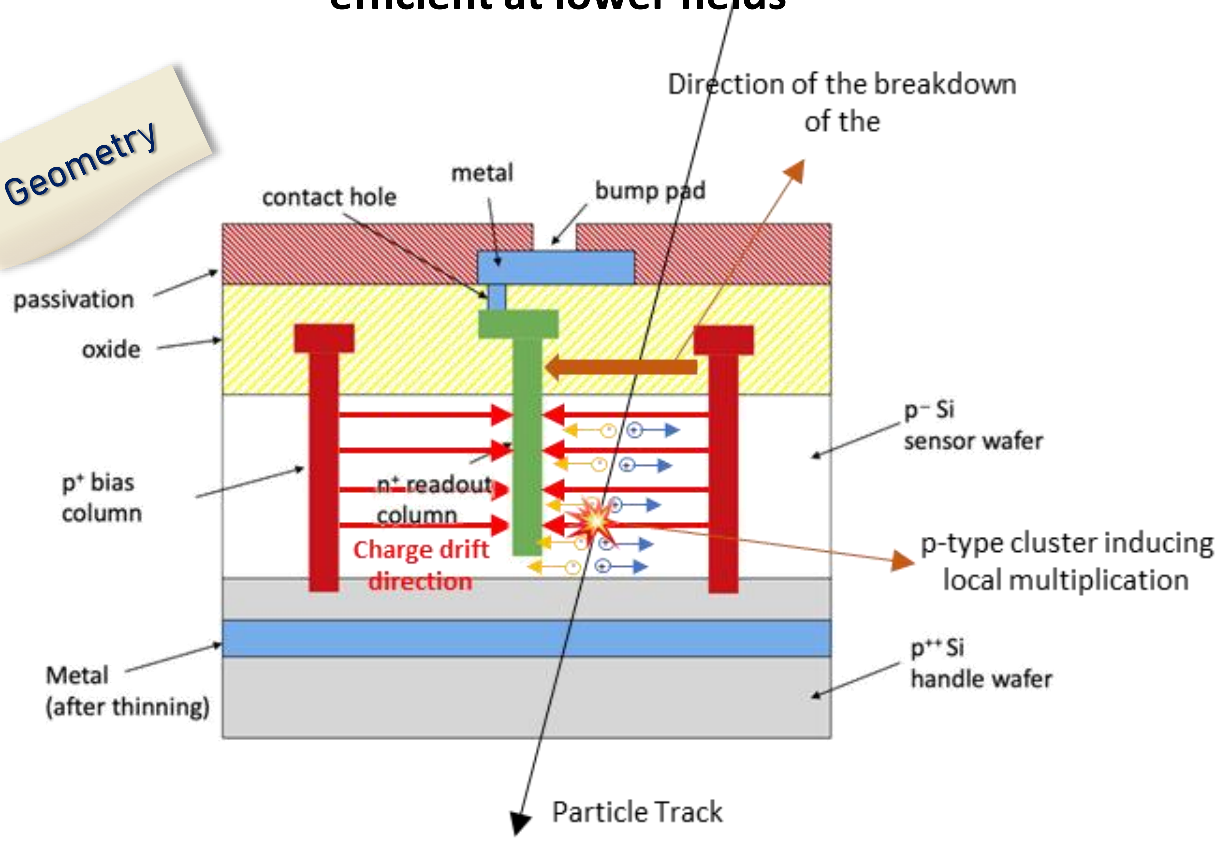

3D Single Pixel structures

Geometry	Irradiation: Species	Irradiation: Flu. (n_{eq}/cm^2)	Operating Conditions	
CNM 13680-6 Single 3D 25 x 100	**Unirradiated**		-50 V	1.4 V/μm
	Fast Neutrons @ JSI	**1×10^{15}**	-180 V	5.1 V/μm
		8×10^{15}	-310 V	8.7 V/μm
		6×10^{16}	-360 V	10.1 V/μm
		1×10^{17}	-410 V	11.5 V/μm
	PS protons (24 GeV/c)	**1×10^{15}**	-210 V	5.9 V/μm
		8×10^{15}	-180 V	5.1 V/μm
CNM 5936-11 Double 3D 55 x 55	**Unirradiated**		60 V	3.2 V/μm
	Fast Neutrons @ JSI	**1×10^{15}**	-160 V	8.5 V/μm
		8×10^{15}	-170 V	9.0 V/μm
		6×10^{16}	-120 V	6.3 V/μm
		1×10^{17}	-200 V	10.6 V/μm
CNM 13680-6 Single 3D 50 x 50	**Unirradiated**		-50 V	2.6 V/μm
	Fast Neutrons @ JSI	**1×10^{15}**	-200 V	10.3 V/μm
		6×10^{16}	-320 V	16.5 V/μm
		1×10^{17}	-340 V	17.6 V/μm
	PS protons	**1×10^{15}**	-180 V	9.3 V/μm